



Norwegian University of
Science and Technology

Handling of Ground Fault in Distribution Networks

Regarding the Field Test Taken by SINTEF in 2005

David Flores

Master of Science in Energy and Environment

Submission date: December 2009

Supervisor: Hans Kristian Høidalen, ELKRAFT

Problem Description

Ground faults are the most common type of faults in power systems and also the most difficult to localize and disconnect. To localize the fault often manual sectionalizing of the network is required. This is time consuming and results in unnecessary outages and reduction in the power quality. Therefore, a detection and location method will be proposed.

The work will be part of a large SINTEF project (Distribution 2020) addressing protection of distribution networks. Part of this large project, a distribution network took place for measurements related to single phase to ground faults. The present work will be taking as main reference the field test.

Tasks

- Modeling the tested Distributed Network in PSCAD.
- Testing in the PSCAD model the Charge Voltage method for detection and location of single to ground faults.

Assignment given: 01. September 2009

Supervisor: Hans Kristian Høidalen, ELKRAFT

DIPLOMA WORK 2009

Norwegian University of Science and Technology, NTNU

Faculty of Natural Sciences and Technology

Department of Power Engineering



Title: Handling Ground Faults in Distribution Networks – Regarding field test taken by SINTEF in August 2005	Subject (3-4 words): Distribution Network, Single phase to ground Fault, concentrated Arc suppression Coil, Petersen Coils, PSCAD.
Author: David Flores	Carried out through: August - December, 2009
Advisor: Professor Hans K. Høidalen, NTNU-Trondheim External advisor: Sen. Scientist Astrid Petterteig, SINTEF Energy Research Center	Number of pages Main report: 76 Appendix: 1
<p>ABSTRACT</p> <p>Goal of work (key words): The main objective of this work was the creation of a PSCAD model, which could be an authentic representative of the distribution network tested by SINTEF and other companies in 2005. Moreover, a new location and detection method for single phase to ground faults is tested throughout the simulations. Most of the simulations were done in a under compensated condition of the system. The zero sequence currents were taken as the most important variables in order to validate the model, throughout a comparison between the field test and simulations values, the validation or not of the model could be made. Finally, consistent shapes related with the QU diagrams are desired between the field test and simulation results, in order to support the validation of the implemented model.</p> <p>Conclusions and recommendations (key words): Consistence was got in all the proposed scenarios. The validation of the model was granted due to the similar results between the field test and simulations. Moreover, the shapes gotten from the QU diagram related to the location and detection method for single phase to ground fault supports the previous statement. It is widely recommended that the interval of time regarding the QU diagram should not be bigger than 3 cycles, during and shortly before the fault. A further research in over compensation should be evaluated in the created PSCAD model as a future work.</p>	
<p style="text-align: center;">1.1 I declare that this is an independent work according to the exam regulations of the Norwegian University of Science and Technology</p> <p style="text-align: center;">  <hr style="width: 20%; margin: auto;"/> Signature </p>	

SUMMARY

The main subject of this master thesis is the study of single phase to ground fault in a given distribution network. SINTEF took part in a field test, which was done in 2005. After the field test being done, a report was elaborated. The report became the main reference of this document. The purpose of this work is the creation of a PSCAD model that can be an authentic representative of the tested distribution network in 2005. Moreover, a detection and location method for single phase to ground faults is tested in order to find any limitation in it and to be an important part of the validation of the model.

The model was created from a variety of given information from SINTEF, a frequency line dependent model was used as a part of the overhead lines representation, in order to have a model as close as possible from the real distribution network behaviour. A deep study of resonant grounding was made in this document, due to its direct involvement in the single phase to ground faults measurements in the field test. The main focus of the model were related to the magnitude and the orientation of the zero sequence currents, the latest ones are considered as the most important variable of study throughout this work.

The validation of the proposed model was granted by the important variables consistency between the field test and the given results from the simulations. The field test results were gotten from the report elaborated by SINTEF. The QU diagrams, which were gotten from the simulations, gave the expected behaviour according to the field test. Therefore, the proposed location and detection method for single phase to ground faults gave an approval to the PSCAD model presented in this document as an authentic representative of the distribution network tested in 2005.

ACKNOWLEDGEMENT

Firstly, I thank God for giving me the skills and determination to complete this important work in my professional career.

I am sincerely grateful to my supervisor, Professor Hans Kristian Høidalen, for giving me the opportunity to develop this interesting and challenging topic. Also, I could not have finished this work without his valuable discussions and suggestions about the theory and the model developed in this work.

I would like to thank, Sen. Scientist Astrid Petterteig for her good and supportive guidance during work. SINTEF Energy Research and Norwegian University of Science and Technology employees for their helpfulness and given facilities, as well as my colleagues, who were with me throughout all these months, in special my colleagues from South America, Alexandra Lucero, Luber Perez and Rafael Vera.

I wish to take this opportunity to express my gratitude to Alexandra Bochmann, for her love and support at every moment until the final end of this work, and to Angel Vargas for his right words at the right moment.

Last but not least, I would like to thank my friends and all my family, specially my parents and my sister for their unconditional support, love and for always believing in me.

TABLE OF CONTENTS

Number of pages	i
1.1 I declare that this is an independent work according to the exam regulations	i
Chapter 1	1
1 INTRODUCTION	1
Chapter 2	3
2 SINGLE PHASE TO GROUND FAULT REPRESENTATION	3
2.1 The positive sequence impedance	4
2.2 The negative sequence impedance	4
2.3 The zero sequence impedance	4
Chapter 3	8
3 SYSTEM GROUNDINGS	8
3.1 Ungrounded or Isolated grounding.....	9
3.1.1 Earth Fault Current and neutral point displacement voltage Analysis.....	10
3.1.2 Fault detection	12
3.2 Solidly grounded system	13
3.2.1 Earth fault current and neutral point voltage analysis.....	13
3.3 Resistance grounded system.....	14
3.3.1 Earth fault current and neutral point voltage displacement analysis.....	16
3.3.2 Fault detection	17
3.4 Resonant grounding.....	18
3.4.1 General aspects of Resonant Grounding Systems.....	19
3.4.2 Principles of the fault current Compensation	20
3.4.3 Earth fault current and neutral point voltage displacement.....	27
Chapter 4	29
4 FAULTY FEEDER IDENTIFICATION BASED ON THE CHARGE VOLTAGE RELATION.....	29
4.1 The ground fault analysis	29
4.1.1 Discharge of the faulty overhead line	30

4.1.2	Charge of the two healthy overhead lines	31
4.1.3	Stationary state of the earth fault.....	33
4.1.4	Approach of the qu method.....	34
Chapter 5	41
5	PSCAD MODEL	41
5.1	Transmission line representation.....	41
5.1.1	Overhead lines.....	42
5.1.2	Cables.....	44
5.1.3	Load Transformers.....	44
5.1.4	Feeder Conductance.....	45
5.2	Substation.....	45
5.3	Henning Feeder.....	46
5.4	Sparbu feeder (FAULTY feeder).....	47
5.5	Sandvollan feeder.....	47
5.6	Special blocks.....	48
5.7	Parameter settings.....	49
5.7.1	Main transformer (Østeras).....	49
5.7.2	Henning Feeder.....	49
5.7.3	Sparbu Feeder.....	50
5.7.4	Sandvollan Feeder.....	50
6	RESULTS	51
6.1	Isolated Condition.....	52
6.2	Resonance curve calculations.....	54
6.2.1	Resonance curve with Parallel resistance connection.....	55
6.2.2	Resonance Curve without Parallel Resistance Connection.....	56
6.3	100% Compensation with Parallel Resistance Connection.....	57
6.4	80% Compensation with Parallel Resistance Connection.....	59
6.5	80% Compensation.....	60
6.6	80% Compensation with Parallel Resistance and High fault Resistance.....	62

6.7	100% Compensation without Parallel Resistance Connection and High Fault Resistance	
	64	
Chapter 7	67
7	DISCUSSION.....	67
Chapter 8	70
8	CONCLUSIONS AND RECOMMENDATIONS.....	70
9	FUTURE WORK.....	72
10	Bibliography.....	73

TABLES

Table 5-1. Main Transformer parameters	49
Table 5-2. Overhead Lines parameters	49
Table 5-3. Cable parameters	50
Table 5-4. Load transformer parameter	50
Table 5-5. Fixed Load parameters	50
Table 5-6. Overhead Lines parameters	50
Table 5-7. Overhead Lines parameters	50
Table 5-8. Cable parameters	50
Table 5-9. Load Transformer parameters.....	50
Table 5-10. Fixed Load parameters	50
Table 6-1. Phasors Magnitude for Isolated Condition	52
Table 6-2. Phasors Angle for Isolated Condition.....	53
Table 6-3. Resonance Curve data.....	55
Table 6-4. Resonance Curve Data.....	56
Table 6-5. Phasors Magnitude with Parallel Resistance Connection.....	57
Table 6-6. Phasors Angle for 100% Compensation with Parallel Resistance Connection	58
Table 6-7. Phasors Magnitude in 80% Compensation with Parallel Resistance Connection	59
Table 6-8. Phasors Angle in 80% Compensation with Parallel Resistance Connection.....	59
Table 6-9. Phasors Magnitude in 80% Compensation System	60
Table 6-10. Phasors Angles in 80% Compensation System	61
Table 6-11. Phasors Magnitud in 80% Compensation with Parallel Resistance and High Fault Resistance	63
Table 6-12. Phasors Angle in 80% Compensation with Parallel Resistance and High Fault Resistance	63
Table 6-13. Phasors Magnitude in 100% Compensation System and High Fault Resistance	65
Table 6-14. Phasors Angle in 100% Compensation System and High Fault Resistance.....	65

LIST OF FIGURES

Figure 2.1: The positive, negative and zero sequence coordinate bases each consists of a set of three phasors 3

Figure 2.2: Circuit Layout of the three phase sequence systems 4

Figure 2.3: Positive, negative and zero sequence networks representing a three phase distribution system 6

Figure 2.4: Positive, negative and zero sequence networks, connected to represent an earth fault.. 6

Figure 3.1: Isolated System..... 9

Figure 3.2: Equivalent circuit of ground fault in an isolated system 10

Figure 3.3: Sequence network equivalent of earth fault in isolated neutral system..... 10

Figure 3.3: Voltage phasors after and before a ground fault in isolated system..... 11

Figure 3.5: Solidly grounded system 13

Figure 3.6: Equivalent circuit of earth fault in solidly grounded system..... 14

Figure 3.6: (a) Phasor diagram for normal operations (b) Phasor diagram for a ground fault 14

Figure 3.8: Resistance grounded system..... 15

Figure 3.9: Sequence network equivalent of an earth fault in a resistance grounded system..... 16

Figure 3.9: Equivalent circuit of an earth fault in resistance grounded system 16

Figure 3.11: Compensated System..... 19

Figure 3.11: Simplified compensated system a) unfaultry b) with a single phase earth fault..... 21

Figure 3.11: Phasor diagrams a) Unfaultry system b) Phase to ground earth fault..... 22

Figure 3.11: Unfaultry compensated system with capacitive and resistive unbalance and damping 24

Figure 3.11. Resonant curve with changing damping and constant k..... 27

Figure 3.16: Sequence network equivalents of ground fault in compensated system 28

Figure 4.1. Discharge of the faulty line over the earth..... 30

Figure 4.2. Change of the voltages during the charging process 31

Figure 3.11. Charging of the two healthy lines over the earth..... 32

Figure 3.11. qu diagram of a low ohmic earth fault..... 36

Figure 3.11. qu diagram of a high ohmic fault..... 36

Figure 3.11. Phase splitting in the healthy network 38

Figure 3.11. a) Single conductor cables in parallel b) Single conductor cables in triangle 39

Figure 3.11. Magnetic coupling of parallel systems 40

Figure 3.11. T-Line Configuration.....	43
Figure 5.2. Overhead Line Topology.....	44
Figure 5.3. Østeras substation Representation.....	45
Figure 5.4. Henning Feeder representation.....	46
Figure 3.11. Sparbu feeder representation.....	47
Figure 5.6. Sandvollan feeder representation.....	48
Figure 3.11. On-line Frequency Scanner (FFT).....	48
Figure 3.11. Phasor-meter.....	49
Figure 6.1. Arc Suppression coil arrangement with parallel resistance.....	51
Figure 6.2. QU Diagram in Isolated System.....	53
Figure 6.3. Resonance Curve with parallel resistance connection.....	56
Figure 6.4. Resonance Curve without parallel resistance connection.....	57
Figure 6.5. QU Diagram in 100% Compensation and Parallel Resistance Connection.....	58
Figure 6.6. QU Diagram in 80% Compensation with Parallel Resistance Connection.....	60
Figure 3.11. QU Diagram in 80% Compensation system.....	62
Figure 6.8. QU Diagram in 80% Compensation with Parallel Resistance Connection and high fault resistance.....	64
Figure 6.9. QU Diagram in 100% Compensation System and High Fault Resistance.....	66

PREFACE

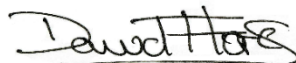
This thesis is part of the diploma work at the Universidad Simon Bolivar – Caracas, Venezuela, Department of Power Engineering; also part of the International Student Exchange Program with the Norwegian University of Science and Technology (NTNU), Trondheim-Norway.

In my fifth and last year of studies in power engineering, I decided to take a new personal experience as an exchange student in Norway, at NTNU, Trondheim. Here, I confronted new challenges in relation to a new culture, a new education system with exams in a different language than my native language. However, most of all was the realization of a research document. All the challenges have been overcome so far, including the last which is fulfilled through this final work.

The theme of the work was study of single phase to ground faults, mainly in resonant grounding. A PSCAD model was developed from a field test, where SINTEF was one of the main companies in the project. The model should have a similar behavior as the real network, where the field test was done. Therefore, certain numbers of cases were implemented in the PSCAD model, in order to compare with the results given by the field test. Moreover, a detection and location method for single phase to ground fault is tested in this model.

During these five months of hard working in this final document, I have been involved with many special persons, who have been very attentive, supportive and helpful during work.

Trondheim, 18th December 2009



Signature

Chapter 1

1 INTRODUCTION

In distribution systems which are not resonant grounded, fault current magnitudes are increasing due to the extension of the underground cable network. Since, the cables can be adapted to higher capacities, underground cables bring about a considerable increase in the magnitude of fault currents with respect to overhead power lines, due to the increasing value of the ground capacitances [1]. Thus, the use of Petersen Coil has been quite used in distribution systems.

Compensated networks (systems with resonant grounding) have gained popularity over the last years in distribution networks. This is mainly due to increased focus on reliability of supply. The number of faults is reduced significantly, and thus running expenses for the utility can be brought down. The arc suppression coil was invented by W. Petersen in 1916 [2] as result of his pioneering work in investigating ground fault phenomena. A well tuned Petersen Coil compensates for the fault current and most arcing faults become self extinguishing. Several methods are utilized in order to detect and located earth faults in compensated networks. However, the not transposed construction of the current Medium Voltage networks increases the challenge for the detection and location methods during faults [3, 4].

If the fault can be located rapidly and accurately, the time of the fault would be shorten and the losses may be reduced greatly, but there are just a few methods for single phase to earth fault location for rural distribution networks, this is one of the main reasons why researches have been done lately in this area [5]. This work will be dealing with a location and detection method named Charge – Voltage Relation, which uses the charge (i.e the integral of the current) rather than the current itself for identifying the faulty feeder. The main reason for their approach is that the charge of the healthy feeders is more or less proportional to the instantaneous value of the zero sequence voltage and the healthy feeders are identified based on the shape of the charge voltage curves [6].

This work could not be possible without the initiative of the project Distribution 2020 – Fault Handling and Integration of Distributed Generation in Medium Voltage network, which aims to develop overall solutions to minimize consequences and costs related to major challenges for the future distribution networks. After the previous project, a field test was done in Østeras Substation by SINTEF and other companies, which are taking part in the project Distribution 2020. A report was developed by SINTEF, the report contents different results obtained in the field test [7], and some more of them are presented in another memo, which was done as well by SINTEF [8], showing details and illustrating the results in alternative ways.

The field test in a rural distribution network was performed in order to expand the distribution project in development. The aim of this document is the creation of a computational model in PSCAD with the purpose of pursuing similar behaviour as the tested rural network. Moreover, the detection and location method is proved in this computational model. The description of the model will be made, after describing important key points in the theory, as the single phase to ground behaviour, system grounding and the proposed detection and location method for single phase to ground faults. Further on, the results from simulation will be presented, in order to have precise conclusions from it.

Chapter 2

2 SINGLE PHASE TO GROUND FAULT REPRESENTATION

In three phase networks short circuits can generally be classified as below, depending on the number of line conductors affected, with or without fault to ground:

- Three phase fault.
- Two phase fault clear of ground.
- Two phase to ground fault.
- Single phase to ground fault.

This work is restricted to single phase to ground fault analysis, in order to perform this study, symmetrical components become a necessary knowledge before analyzing the single phase to ground behaviour in different kind of grounding. Calculation with symmetrical components will be described, in the following.

The description of this chapter is based on [9], [10], [11] and [12].

The use of symmetrical components is a mathematical method that is based on a change of the system of coordinates. It involves a transformation from Phase coordinates to sequence coordinates a_1 , a_2 and a_3 as it is shown in the Figure 2.1.

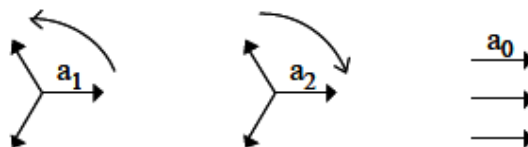


Figure 2.1: The positive, negative and zero sequence coordinate bases each consists of a set of three phasors

In accordance with the definitions of the systems the effective impedances for the different components are called the positive sequence, negative sequence and zero sequence impedances. The next figure shows the circuit layouts of the individual networks for measurement of the impedance values. For short circuit studies, symmetrical three phase voltages are used for the positive sequence and negative sequence systems, and a single phase voltage source for the zero sequence system.

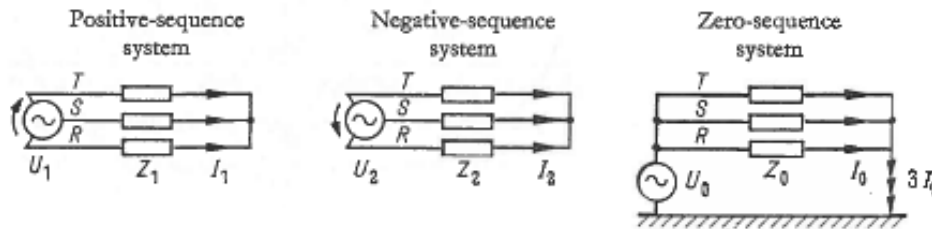


Figure 2.2: Circuit Layout of the three phase sequence systems

2.1 The positive sequence impedance

The positive sequence impedance z_1 is the impedance of the items of plant, equipment and lines measured under balance load conditions. It is therefore equal to the per phase impedance of the lines, the short circuit impedance of the transformers and reactors and the effective generator impedance at the instant of occurrence of the short circuit.

2.2 The negative sequence impedance

The negative sequence impedance z_2 for lines, transformers and reactors is the same as the positive sequence impedance, because the impedance of these is unchanged if a symmetrical voltage system with reverse sequence is applied to them.

2.3 The zero sequence impedance

The zero sequence impedance z_0 can be determined by measurement or calculation, the three phases of the three phase network being connected in parallel and a single phase alternating voltage applied to them. Generators usually have a very much smaller zero sequence impedance than the sub transient reactance. The value of the zero sequence impedance of transformer depends on the kind of connection. Star-delta transformers have a zero sequence impedance from about 0.8 to 1 time the positive sequence impedance. Star-star transformers without tertiary windings have a zero sequence impedance of about five to ten times the positive sequence impedance. Because of the large leakage flux flowing through the transformer tank walls and consequent heating they are not generally suitable for system grounding. In the case of shell type transformers and banks of three single phase transformer in star-star connection the zero sequence impedance is of about the same order as the open circuit impedance because of the free magnetic return path. They are therefore unsuitable for system grounding.

The zero sequence impedance of lines depends greatly on the kind of transmission (overhead lines or cables) and the electrical conductivity of the soil. The three currents of the zero sequence system, equal in magnitude and direction, are opposed by an impedance which in the case of overhead lines result from the loop constituted by the three line conductors and earth and in the case of cables by the loops constituted by the three cable cores, lead sheath and earth. The zero sequence reactance of overhead lines is about 3 to 3.5 times greater than the positive sequence reactance depending on the conductor section and conductor arrangement. The effective (a.c.) resistance of the zero sequence system includes both the effective resistance of the line conductor and that of the earth return. The latter necessitates an addition of about $0.15 \Omega/km$ to the effective resistance of the conductor, the ground resistivity may change according to the type of soil.

In the case of overhead lines with earth wires part of the zero sequence current also flows back through the earth wires. The use of steel earth wires does not significantly reduce the zero sequence reactance, but there is a marked reduction when earth wires with good conductivity, e.g. of steel cored aluminium or copper, are employed.

The zero sequence impedance of cables differs much more from the positive sequence impedance than with overhead lines because of the widely differing influence of the lead sheath. Belted cables

have a higher zero sequence reactance than three core cables with separately lead covered cores (SL cables), which in turn have a higher zero sequence reactance than single core cables. The effective (a.c.) resistance of the zero sequence system includes both the effective resistance of the cable cores and that of the lead sheaths, whereby it is increased several times.

The single phase to ground fault analysis is performed by transforming the three phase network into positive, negative and zero sequence networks, as it was previously explained. The sequence networks can each be represented by a two terminal network. The positive, negative and zero sequence two terminal equivalents are shown in the next figure. In three phase systems, all voltages are generated in the positive sequence network and consequently, the negative and zero sequence two terminal networks only consist of the equivalent impedances.

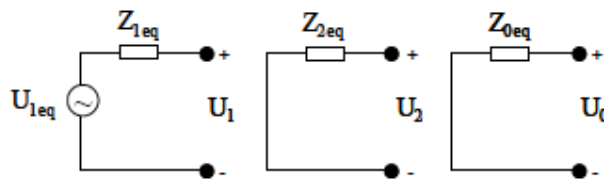


Figure 2.3: Positive, negative and zero sequence networks representing a three phase distribution system

The Figure 2.4 shows a series connection of the sequence networks, which represents a single phase to ground fault.

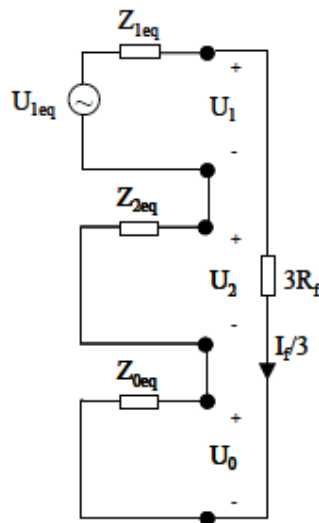


Figure 2.4: Positive, negative and zero sequence networks, connected to represent an earth fault

During an earth fault, the three sequence currents equal each other at the fault location. The total fault current I_f is the sum of the sequence currents and thereby three times the positive, negative or zero sequence current. The fault impedance R_f must be multiplied by three to be properly represented in the sequence network connection, according to the previous figure.

Chapter 3

3 SYSTEM GROUNDINGS

The system grounding is the combination of components that are used to control the behaviour of system parameters at the moment of any asymmetry in the network. In practice, the system grounding consists of connections between transformer neutral points and earth.

The kind of system grounding influences the zero sequence equivalent impedance of the system and by that, the unsymmetrical fault current, which determines the voltage at the transformer neutral, that is to say, the neutral point displacement voltage.

The main goals of system grounding are to minimize voltage and thermal stresses on equipment, provide personnel safety, reduce communications system interference, and give assistance in rapid detection and elimination of ground faults.

With the exception of voltage stress, operation a system as ungrounded, high-impedance grounded or resonant grounded restricts ground fault current magnitudes and achieves most of the goals listed above. The drawback of these grounding methods is that they also create fault detection (protection) sensitivity problems. We can create a system grounding that reduces voltage stress at the cost of large fault current magnitudes. However, in such a system the faulted circuit must be de-energized immediately to avoid thermal stress, communications channel interference, and human safety hazards. The disadvantage of this system is that service must be interrupted even for temporary faults.

The following is a brief description of the grounding methods typically used in medium voltage networks, doing special focus in Isolated Neutral and Resonant grounding.

3.1 Ungrounded or Isolated grounding

Provided the safety requirements are fulfilled, the system grounding shall be designed to keep associated costs as low as possible. The easiest and cheapest method for system grounding is to leave the transformer neutral points isolated. Figure 3.1 shows an earth fault in an isolated system.

The description of this chapter is mainly based on [10] and [13].

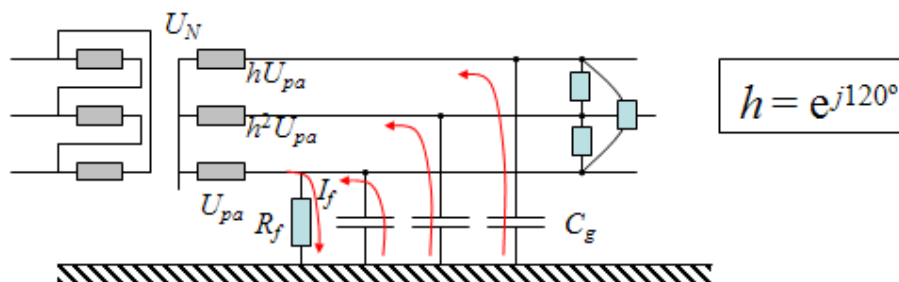


Figure 3.1: Isolated System

In conventional systems consisting of overhead lines and short cables, the series impedance is very small compared to the shunt impedance and does not influence the earth fault behaviour. It can therefore be neglected in the three phase equivalent circuit shown.

In an isolated neutral system (see Figure 3.1), the neutral has no intentional connection to ground: the system is connected to ground through the line to ground capacitances. Single line to ground faults shift the system neutral voltage but leave the phase to phase voltage triangle intact.

For these systems, two major ground fault current magnitude limiting factors are the zero sequence line to ground capacitance and fault resistance as it could be seen in the equivalent circuit of earth fault (Figure 3.2). Because the voltage triangle is relatively undisturbed, these systems can remain operational during sustained, low magnitude faults.

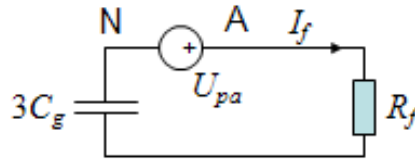


Figure 3.2: Equivalent circuit of ground fault in an isolated system

3.1.1 Earth Fault Current and neutral point displacement voltage Analysis

The fault current and the neutral point displacement voltage can be derived from the equivalent circuit in Figure 3.3 or the sequence network equivalent in the upcoming figure.

Both the current and the voltage reach their maximum values during a solid earth fault, i.e when the fault resistance is zero. In this case, the fault current will be limited by the capacitance and the fault resistance:

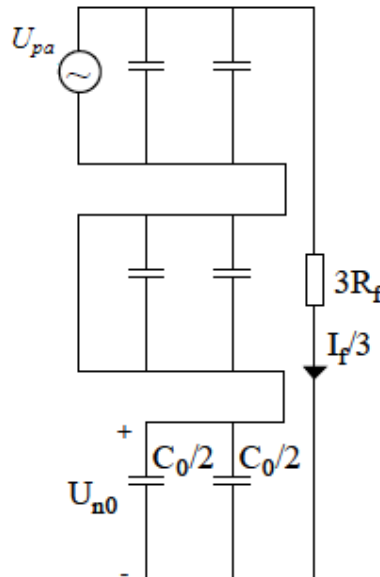


Figure 3.3: Sequence network equivalent of earth fault in isolated neutral system

$$I_f = 3 \frac{U_{pa}}{3R_f + \frac{1}{j\omega C_g}} \tag{3.1}$$

$$I_f = \frac{U_{pa} \cdot 3j\omega C_g}{1 + 3j\omega C_g R_f} \quad 3.2$$

In the special case of $R_f = 0 \Omega$. The fault current becomes:

$$I_f = 3I_0 = 3j\omega C_g U_{pa} \quad 3.3$$

Throughout the previous expression, it could be seen that the fault current is proportional to the total capacitive connection to earth. If the capacitance of the system is strong, the magnitude of the fault current will be therefore large and possibly dangerous. If the maximum earth fault current is considered dangerous, an isolated neutral system is not sufficient to fulfill the safety regulations and a different system grounding is required.

The voltages between the neutral point and the healthy phases are not influenced by the earth fault. The next figure shows how the magnitudes of the line voltages and line to ground voltages after a single phase to ground fault is applied.

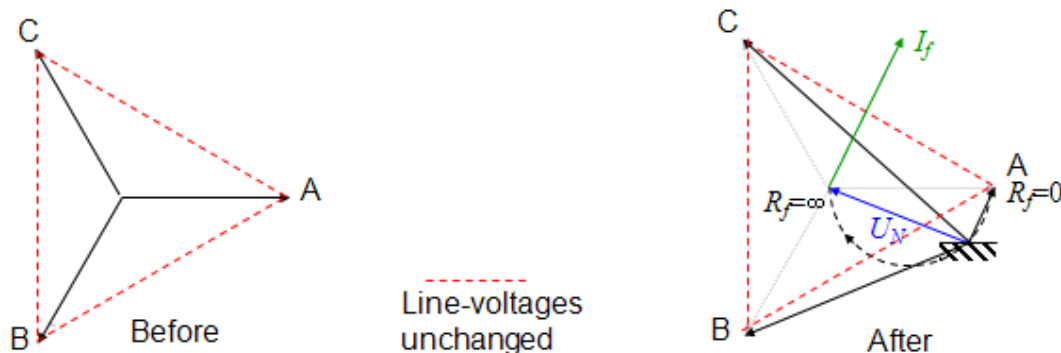


Figure 3.4: Voltage phasors after and before a ground fault in isolated system

The presence of a fault resistance increases the equivalent impedance of the system. This decreases the magnitude of the fault current as well as the magnitude of the neutral point displacement voltage.

The fault resistance adds a resistive part to the equivalent impedance and the earth fault current therefore consists of a resistive as well as reactive component:

$$I_f = I_R + jI_C = \frac{R_f(3\omega C_g)^2 U_{pa}}{1 + (R_f 3\omega C_g)^2} + j \frac{3\omega C_g U_{pa}}{1 + (R_f 3\omega C_g)^2} \quad 3.4$$

Since there is a voltage drop across the fault resistance, the entire pre fault phase voltage is not applied across the system capacitance. The neutral point displacement voltage does not equal the pre fault phase voltage but is instead determined by the relation between the zero sequence impedance and the fault resistance, as it could be deduced from the Figure 3.2.

$$U_N = U_0 = \frac{-U_{pa}}{1 + 3j\omega C_g R_f} = \frac{-I_f}{3j\omega C_g} \quad 3.5$$

Even though the neutral point displacement voltage does not reach the pre fault phase voltage value, it differs from zero, and the magnitude of the voltage of the healthy phases might still exceed the pre fault values, as it could be appreciated in the Figure 3.2. The phase and the magnitude of the neutral point voltage and the voltage across the fault resistance depend on the phase and magnitude of the earth fault current, and the fault resistance.

3.1.2 Fault detection

If the unsymmetrical current and the neutral point displacement voltage measured during earth faults differ sufficiently from normal operation values, they can be used to detect earth faults in the system. Typically, over voltage relays are used to detect the neutral point displacement voltage and directional residual over current relays are used for selective fault detection.

The relay settings, i.e. the relay operation thresholds, decide the sensitivity of the ground fault detection. Since high-impedance faults give relatively low fault currents and neutral point displacement voltages, high-impedance fault detection requires low relay operation thresholds. However, there are always natural unbalances in the systems. Natural unbalances give rise to a neutral point displacement voltage and unsymmetrical currents equivalent to those of very high-impedance faults. The voltage and currents can cause unwanted relay operation during normal operation if the thresholds are set too low.

If an acceptable balance between the desired detection and natural unbalances cannot be reached, different system grounding is required.

Isolated neutral grounding might lead to high fault currents in systems with very strong capacitance and is therefore not a suitable grounding method in system with extensive use of cable. As it might also lead to insufficient fault detection in systems with very weak capacitance, it is neither suitable as a system grounding in small networks consisting of overhead lines.

3.2 Solidly grounded system

To be classified as solidly grounded system, the system must have $(X_0/X_1) \leq 3$ and $(R_0/X_1) \leq 1$, where X_0 and R_0 are the zero sequence reactance and resistance, and X_1 is the positive reactance of the system [14]. In practice, solidly grounded systems have all power system neutrals connected to earth (or ground) without any intentional impedance between the neutral and earth.

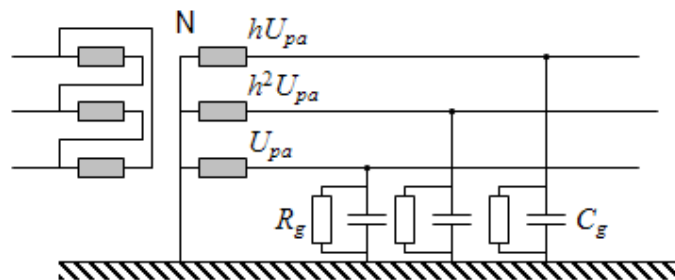


Figure 3.5: Solidly grounded system

3.2.1 Earth fault current and neutral point voltage analysis

Ground faults on these systems may produce high magnitude currents that require tripping the entire circuit and interruption load to many customers. About 80 per cent of ground fault occurring on overhead distribution lines are transient. For these systems automatic multishot reclosing is widely used. The resulting interruption/restoration cycle can represent a problem to customers with large rotating loads or those with loads intolerant of voltage sags.

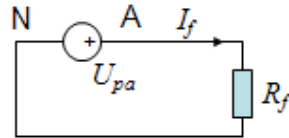


Figure 3.6: Equivalent circuit of earth fault in solidly grounded system

In Figure 3.6, the fault current in solidly grounded systems is limited only by the fault resistance and by the series impedance from the transformer or the line, which in this case was neglected.

Solid grounding reduces the risk of over voltages during ground faults. These faults do not shift the system neutral (see next figure). Thus, the system does not require as high a voltage insulation level as does an isolated neutral system. Transmission systems are typically solidly grounded throughout the world.

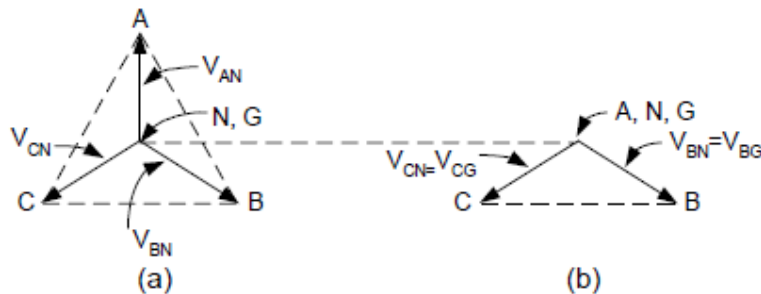


Figure 3.7: (a) Phasor diagram for normal operations (b) Phasor diagram for a ground fault

The typical ground fault protection for solidly grounded systems consists of residually connected (or equivalent mathematical summation) non directional and directional over current relays.

3.3 Resistance grounded system

In order to facilitate high impedance earth fault detection in systems with weak capacitive connection to earth, the difference between high impedance earth fault currents and voltages, and those during normal operation must be increased. One way to increase the margin between high impedance earth fault currents and currents due to normal operation unbalances is to connect a

neutral point resistance to the neutral points of some of the transformers in the system. The upcoming figure shows an earth fault in a system with a resistance grounded neutral.

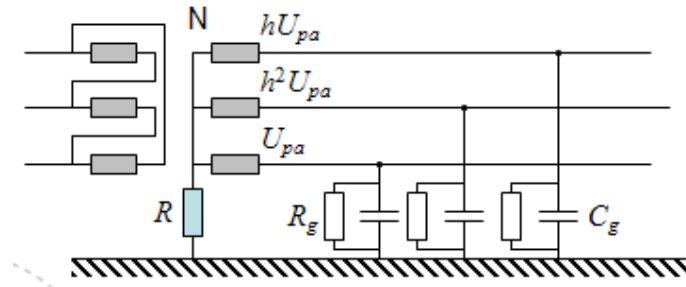


Figure 3.8: Resistance grounded system

The resistor used in this kind of grounded system can be a high resistance as well as a low resistance. The high resistance is used in order to limit transients over voltages and currents to safe values during ground faults. Meanwhile the low resistance has objective of limiting the ground fault current, in that way the thermal stress is reduced and less expensive switchgear can be bought.

Typical fields of application for resistance grounding include generators connected in a generator transformer unit [14] and medium voltage industrial plant distribution networks [15].

The Figure 3.9 will show the corresponding sequence networks equivalent. Since conventional distribution system is assumed, the series impedance is neglected in the next two equivalent circuits.

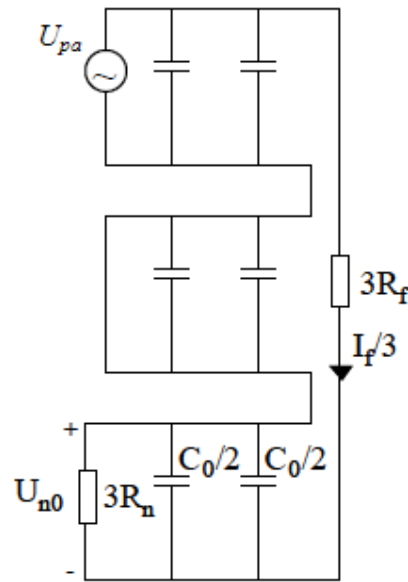


Figure 3.9: Sequence network equivalent of an earth fault in a resistance grounded system

Since the neutral point resistance is parallel to the equivalent capacitance of the system, it decreases the magnitude of the resulting equivalent impedance and shifts its phase. These changes of equivalent system impedance magnitude and phase influence both the low and the high impedance earth fault behaviour of the system. Therefore, the next figure will show the equivalent circuit of an earth fault in resistance grounded system.

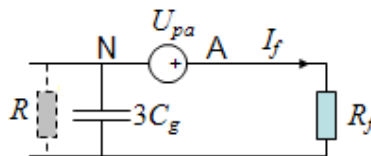


Figure 3.10: Equivalent circuit of an earth fault in resistance grounded system

3.3.1 Earth fault current and neutral point voltage displacement analysis

The maximum earth fault current in resistance grounded system consists of a resistive as well as a reactive component, in this section the fault resistance has been neglected.

$$I_f = I_R + jI_C = \frac{U_{pa}}{R_n} + j3\omega C_g U_{pa} \tag{3.6}$$

In overhead line systems with weak capacitive connection to earth, the capacitive shunt reactance is very large compare to the parallel neutral point resistance and the maximum earth fault current is therefore determined almost exclusively by the neutral point resistance:

$$\frac{1}{R_N} \gg 3\omega C_g \Rightarrow I_f \approx \frac{U_{pa}}{R_n} \quad 3.7$$

From figure 1-7, the neutral point voltage can be expressed

$$U_N = -U_{pa} \quad 3.8$$

3.3.2 Fault detection

A fault resistance reduces the magnitude of the fault current. In resistance grounded systems with weak capacitive connection to ground, the phase of the current is however unaffected and the current solely resistive:

$$I_f = \frac{U_{pa}}{R_n + R_f} \quad 3.9$$

Since the neutral point resistance decreases the zero sequence impedance, the amplitude of the earth fault current will look like the amplitude of the earth fault current in isolated neutral systems with much higher capacitive connection to earth. Consequently, small overhead line systems with weak capacitive connection to earth can be resistance grounded in order to facilitate earth fault detection [10].

Nonselective ground fault detection is possible by sensing system zero sequence voltage magnitude and comparing it with an overvoltage threshold, or by measuring all three phase to ground voltages and comparing each voltage magnitude against an under voltage threshold. To find the faulted feeder, you must use sensitive zero sequence directional elements or disconnect feeders to determine when the zero sequence voltage drops to a normal level

3.4 Resonant grounding

According to [16], Experience with resonant grounding has been very satisfactory. The equipment requires practically no maintenance and hardly any attention since detuning is permissible within reasonable margins, according to the network topology. The major field of application of resonant grounding is at voltages of 69 kV and below. Operation on sustained faults has been successful in many systems for hours and even days. Therefore, one way of improving power quality is to use resonant grounding whereby the compensatory effect of the coil minimizes the fault current and allows service to be maintained during a fault. The disadvantage is the difficulty of selective fault detection, which is, in fact, due to the low levels of fault currents.

In not resonant grounded distribution systems, fault current magnitudes are increasing due to the extension of the underground cable network. Since, the cables can cope with higher capacities, therefore, the ground capacitance may be higher, underground cables bring about a considerable increase in the magnitude of fault currents with respect to overhead power lines. Thus, relatively short underground cable lengths may have a considerable effect on the magnitude of the fault current in medium voltage systems.

During normal system operation, the grounding method does not have a relevant impact. However, consequences of single phase faults on the system depend to a large extent on the grounding method chosen. In systems with low impedance grounding, these single phase faults cause considerable fault current, requiring complex grounding facilities; at the same time, these large currents allow the faults to be detected and cleared quickly. In the case of grounding using a resonant coil, the fault current is reduced to a minimum, because the inductive reactance of the coil compensates the capacitive reactance of the system at all times. Using resonant grounded systems, transient outages are automatically cancelled (normally self extinguished arcs) without response of the switches or fuses within the system; therefore, the service is not interrupted. Thus, supply may be maintained during the fault. Some comment should be made of the facts that this methodology is used in countries in northern and central Europe and that research to this end is being carried out in France, Italy and the United Kingdom, countries that are not traditional users of the resonant grounding system.

3.4.1 General aspects of Resonant Grounding Systems

A resonant grounding system has a variable single phase reactance (Arc Suppression Coil or Petersen Coil), connected between the neutral of a transformer and the earth. The inductive current of the coil cancels the capacitive fault current so that the current, which circulates through the fault point, is reduced to a small resistive component. This residual current is originated by the conductances in parallel with the grounding capacities of the system, the losses of the coil itself, and the resistance of the arc.

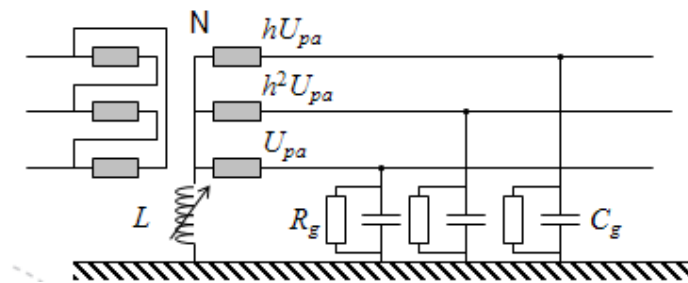


Figure 3.11: Compensated System

Some of the most important advantages of using the resonant coil as grounding method are as follows [17]:

- Compensation of the fault current reduces the current to a level that the values established by electrical safety regulations for increases in the grounding voltage can be achieved at a reasonable cost for grounding.
- The number of high speed automatic re-closures caused by ground faults is reduced by between 70 and 90 per cent, thus reducing the number of transitory clearances in a network.
- The need for maintenance of the switches is reduced.
- The voltage increase after extinction of the arc is slow, thus reducing the risk of restarting the arc.
- In single phase fault conditions in the system, it is possible to operate for a space of several hours, even when the fault persists.
- When the network operates in permanent fault conditions, the power dissipated in the fault is very small due to the compensation.

- The compensation reduces the possibility that a single phase fault develops into other types of faults (double phase or three phase) due to the self extinguishing effect exerted by the compensation.

However, this method of grounding also involves the following drawbacks.

- In protection systems using traditional technology, the reliability and sensitivity of relays is reduced.
- The difficulty of locating faults is increased.
- During the ground fault, voltages in the sound phases increase by square three ($\sqrt{3}$). It limits implementation of this type of grounding to intermediary voltage systems. It would not be economically viable, because of the investment required in the insulation to implement it on higher voltage levels.
- The probability of double ground faults increases in weak points in the system due to the voltage increase experienced.

3.4.2 Principles of the fault current Compensation

In order to demonstrate the principle of fault current compensation, the simplified system shown in the next figure is considered. The power system and the voltage source are supposed to be symmetrical and linear; reactances of the line and of the voltage sources are neglected in a first step. The system is ungrounded and only the steady state at the nominal frequency will be considered, neglecting all transient phenomena and harmonics. The latter simplification will apply for all considerations developed below.

This section is based on [1].

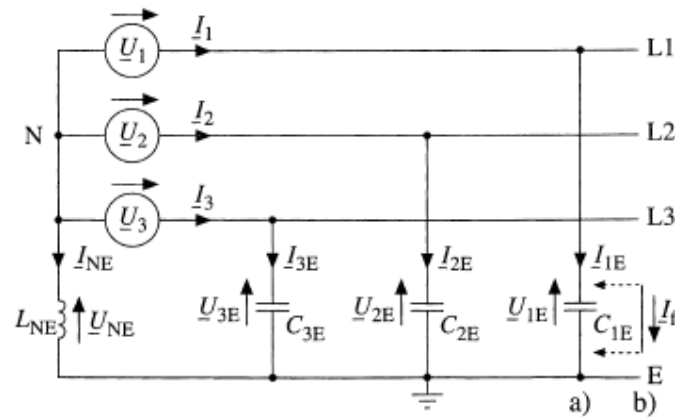


Figure 3.12: Simplified compensated system a) unfaulty b) with a single phase earth fault

The remaining parts of the system are the symmetrical voltage source U_1, U_2, U_3 , the phase to ground capacitances C_{1E}, C_{2E}, C_{3E} and the inductance between the neutral and ground L_{NE} .

First, the unfaulty system Figure 3.12: is considered. The Phasor diagram for this case is shown in Figure 3.13: . Since the system is supposed to be symmetrical, the vector sum of the capacitive earth current and, consequently, the current in the neutral inductance, I_{NE} equals zero:

$$I_{NE} = -(I_{1E} + I_{2E} + I_{3E}) = 0 \quad 3.10$$

Hence, the neutral to ground voltage U_{NE} is zero as well, the potential of the neutral being equal to the ground potential.

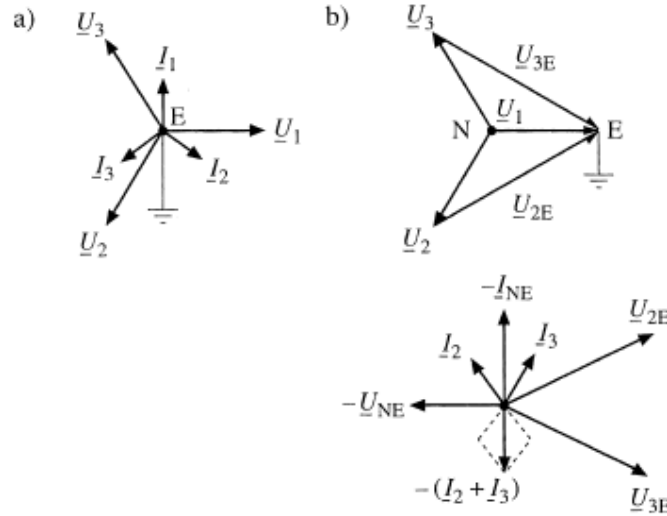


Figure 3.13: Phasor diagrams a) Unfaultry system b) Phase to ground earth fault

So far, the grounding method of the neutral is not important. This changes if a single phase earth fault is considered between, e.g., phase 1 and ground. In this case, the potential of the faulty phase is identical with the ground potential. The voltage between the two healthy phases and ground is increased and the voltage between the neutral and ground becomes the inverse of the faulty phase source voltage. The Phasor diagram of this configuration is shown in Figure 3.13. The fault current is given by the vector sum of the current in the neutral inductance and the capacitive earth currents of the two healthy phases:

$$I_f = I_{1E} = -I_{NE} - (I_{2E} + I_{3E}) \quad 3.11$$

Hence, as can be seen in the vector diagram, the current in the neutral inductance ($-I_{NE}$) and the resulting capacitive earth current of the healthy phases ($I_{2E} + I_{3E}$) are opposite to each other. It is thus possible to obtain a zero fault current by adjusting the magnitudes of the two currents properly. The capacitive earth current depends on the topology of the system and cannot be influenced. On the other hand, the magnitude of the neutral current I_{NE} depends on the value of the neutral inductance and therefore can be modified. Considering the inductive neutral to ground current to compensate the capacitive phase current leads to the names **compensated system** and **earth fault compensation** and to the following definitions:

$$|I_{NE}| \begin{cases} > \\ = \\ < \end{cases} |I_{2E} + I_{3E}|: \text{the system is } \begin{cases} \text{Over compensated} \\ \text{Compensated or Tuned} \\ \text{Under compensated} \end{cases}$$

If the system is exactly tuned, the fault current is zero. Earth faults due to arcs can not subsist since there is no recovery voltage to maintain the conducting channel. Therefore, these faults will disappear immediately after their occurrence [18]. For all other single phase earth faults, the fault current is very small (0.1A ... 5A).

The simplifications assumed in this paragraph to explain the principle of resonant grounded system do not always represent the physical system with enough accuracy. In order to explain some phenomena observed in unfaultry compensated system, in particular a relatively high neutral to ground voltage, the theory expose in the following paragraph has been developed.

3.4.2.1 Basic theory

The system shown in the next figure is considered. The voltage sources are still supposed to be symmetrical, and the system is unloaded and linear. Due to the geometry of the line, the phase to ground capacitances of the three phases C_{1E}, C_{2E}, C_{3E} are slightly different.

The resistances of the neutral coil windings and the phase to ground resistances R_{1E}, R_{2E}, R_{3E} are also taken into account. The case $R_{1E} \neq R_{2E} \neq R_{3E}$ is already and extension of the basic theory; the references assume either $R_{1E} = R_{2E} = R_{3E}$ or neglect the influence of the phase to ground resistances ($R_{1E} = R_{2E} = R_{3E} \rightarrow \infty$).

Using a complex notation of the voltage vectors, the voltages of the symmetrical source can be written as follows:

$$\begin{aligned} U_1 &= U_{nom} \\ U_2 &= a^2 U_{nom} \\ U_3 &= a U_{nom} \end{aligned} \tag{3.12}$$

In the previous equations the quantity U_{nom} is rated rms phase to neutral voltage of the power source and a^2 and a are rotation operators in the complex plane:

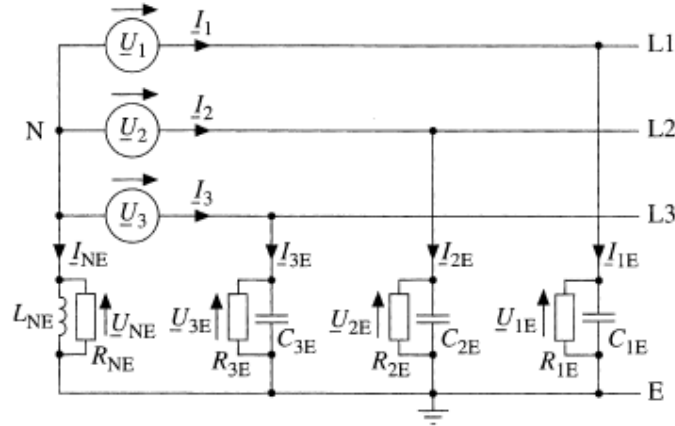


Figure 3.14: Unfaulty compensated system with capacitive and resistive unbalance and damping

$$a = e^{j2\pi/3} = -\frac{1}{2} + j\frac{\sqrt{3}}{2}$$

3.13

$$a^2 = e^{j4\pi/3} = -\frac{1}{2} - j\frac{\sqrt{3}}{2}$$

The normalized neutral to ground voltage of the system is:

$$u_{NE} = \frac{U_{NE}}{U_{nom}} = -\left\{ j\omega C_{1E} + a^2 j\omega C_{2E} + a j\omega C_{3E} + \frac{1}{R_{1E}} + a^2 \frac{1}{R_{2E}} + a \frac{1}{R_{3E}} \right\} \cdot \left\{ \frac{1}{j\omega L_{NE}} + j\omega C_{1E} + j\omega C_{2E} + j\omega C_{3E} + \frac{1}{R_{1E}} + \frac{1}{R_{2E}} + \frac{1}{R_{3E}} + \frac{1}{R_{NE}} \right\}^{-1} \quad 3.14$$

It is possible to simplify the above equation by introducing the following key parameters

- Mismatch m

$$m = \frac{\frac{1}{j\omega L_{NE}} - j\omega C_{tE}}{j\omega C_{tE}} \quad 3.15$$

Where C_{tE} represents the total phase to ground capacitance of the system:

$$C_{tE} = C_{1E} + C_{2E} + C_{3E}$$

And ω the rated angular frequency:

$$\omega = 2\pi f_{nom}$$

The mismatch m indicates the degree of tuning of the system. Referring previously

$$|I_{NE}| \begin{cases} > \\ = \\ < \end{cases} |I_{2E} + I_{3E}| : \text{the system is } \begin{cases} \text{Over compensated} \\ \text{Compensated or Tuned} \\ \text{Under compensated} \end{cases}$$

Note that for $L_{NE} \rightarrow \infty$, i.e. the absence of an inductive part in the neutral to ground connection, m becomes -1. This case represents a resistively grounded system. On the other hand, for $L_{NE} \rightarrow 0$, i.e. a directly grounded system, $m \rightarrow +\infty$. It applies

$$-1 \leq m \leq +\infty \quad 3.16$$

o Unbalance k

$$k = k_c + k_r \quad 3.17$$

Where k_c is the capacitive part of the unbalance

$$k_c = \frac{C_{1E} + a^2 C_{2E} + a C_{3E}}{C_{tE}} \quad 3.18$$

And k_r is the resistive part of the unbalance

$$k_r = -j \frac{1/R_{1E} + a^2 1/R_{2E} + a 1/R_{3E}}{\omega C_{tE}} \quad 3.19$$

The normalize complex parameter k indicates the phase and the magnitude of the asymmetry of the three phases to ground. Its value depends on the topology and the nature of the system (overhead lines, cables, etc) E.g., capacitive coupling to neighboring lines can influence the virtual phase to ground capacitances. The typical value of $|k|$ varies between 0.001 and 0.03.

Using only the neutral to ground voltage and the neutral current, it is not possible to determine the parts k_C and k_r of k . It is, however, normally supposed that the unbalance is mainly due to a capacitive asymmetry of the system.

- Damping d

$$d = \frac{1}{R_{tE} \omega C_{tE}} \quad 3.20$$

Where

$$\frac{1}{R_{tE}} = \frac{1}{R_{1E}} + \frac{1}{R_{2E}} + \frac{1}{R_{3E}} \quad 3.21$$

If $R_{tE} \ll R_{1E}, R_{2E}, R_{3E}$, $R_{tE} \approx R_{NE}$ applies approximatively for an unfaulty system.

The value of d can vary in a wide range, depending on the system and on the implemented neutral to ground admittance. The typical value of d varies between 0.001 and 0.05.

The circuit containing the elements L_{NE} , C_{tE} , and R_{tE} can be considered as a parallel oscillatory circuit. This explains the denotations **damping**, **tuning**, **mismatch** and **resonant earth system**.

All parameters are subject to natural changes due to variations for e.g. humidity and temperature. They change as well if parts of the system are connected or disconnected. Using the above defined parameters, the normalized neutral to ground voltage u_{NE} can be written as follows:

$$u_{NE} = \frac{U_{NE}}{U_{nom}} = \frac{k}{m + jd} \quad 3.22$$

The previous equation shows the influence of the parameters unbalance k , mismatch m and damping d on the normalized neutral to ground voltage. The maximum of this curve is at $m = 0$, i.e. the system is exactly tuned. Thus, a complete compensation of the capacitive fault current under fault conditions means a maximal magnitude of the neutral to ground voltage under normal conditions. If $|k|$ is large and the damping d is low, the maximum of the resonant curve can be greater than the nominal voltage. Therefore, care has to be taken in designing the neutral admittance. If the system is

known to have a low damping and to be very unbalanced, the resistive part of the neutral admittance should be increased. One example of this is represented in the next figure

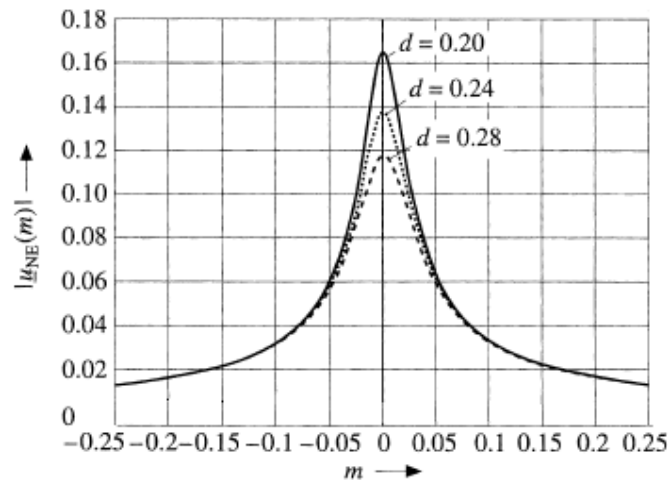


Figure 3.15. Resonant curve with changing damping and constant k

The equation of the resonant curve can be derived from the previous equation:

$$|u_{NE}| = \frac{|k|}{\sqrt{m^2 + d^2}} \quad 3.23$$

It is known that the neutral to ground voltage allows tuning the neutral impedance of a compensated system using the resonance curve method. This principle is widely used.

It is convenient to remember that the tuning of the system throughout the neutral to ground voltage is made, when there is not any fault in the network.

3.4.3 Earth fault current and neutral point voltage displacement

In resonant grounded systems, the earth fault current is decreased by use of inductive neutral point reactors called Petersen coils. The Petersen coils, which are connected between an arbitrary number of the transformer neutral points and earth, decrease the resulting capacitive strength of the system.

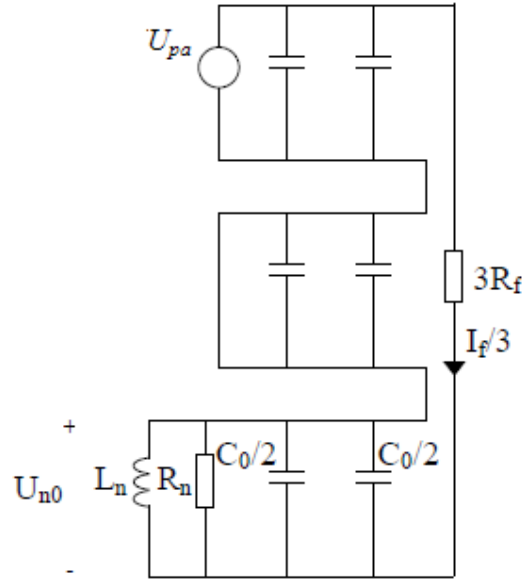


Figure 3.16: Sequence network equivalents of ground fault in compensated system

The Figure 3.16 shows the corresponding equivalent circuit in a system with negligible series of impedance. The equivalent reactance of a resonance earthed system is the parallel connection of the capacitance to earth and the neutral point inductance:

$$X_0 = \frac{\frac{1}{3\omega C_g} \cdot \omega L_N}{\frac{1}{3\omega C_g} + \omega L_N} = \frac{\omega L_N}{1 + \omega^2 L_N 3C_g} \quad 3.24$$

If the size of the Petersen coil reactance is of the same size as the capacitive reactance of the system, the resulting impedance is very large and the ground fault current small at the fault location. In order to facilitate earth fault detection, the neutral point reactor can be combined with a neutral point resistor. The equivalent impedance of the system is then the parallel connection of the reactance and the neutral point resistance.

$$Z_0 = \frac{R_n \cdot j \cdot X_0}{R_n + j \cdot X_0} \quad 3.25$$

Chapter 4**4 FAULTY FEEDER IDENTIFICATION BASED ON THE CHARGE VOLTAGE RELATION**

In many countries of Europe, the resonant grounding is one of the most important options in electrical network design to obtain the optimal power supply quality, as we have pointed out previously in this work. The main advantage of the treatment of the neutral point is the possibility of continuing the network operation during a sustained ground fault. As a consequence this reduces the number of interruptions of the power supply for the customer.

A single phase to ground fault in a network that is isolated or grounded by an arc suppression coil causes a rather low fault current and the faulty feeder is traditionally identified from the zero sequence voltage and the sum of the phase currents fed into each feeder from the bus bar. An alternative proposed in the literature using the charge (i.e. the integral of the current) rather than the current itself from identifying the faulty feeder. The main reason for the proposed approach is that the charge of the healthy feeders is more or less proportional to the instantaneous value of the zero sequence voltage in both transient and steady state conditions. The healthy feeders are identified based on the shape of the charge-voltage curves.

The description of this chapter is based on [19], [20] and [6]

4.1 The ground fault analysis

To explain the behavior of a single phase to ground fault, three different processes can be superposed. All three processes are starting at the same time, but their duration is different.

It can be distinguished between the following processes:

- Discharge of the faulty line overhead line.

- Charging of the two healthy overhead line.
- Stationary state of the earth fault.

The explanation of the three processes will be made by using a network with three feeders (A,B and C) and an earth fault in line 1 of feeder A according to the next figure.

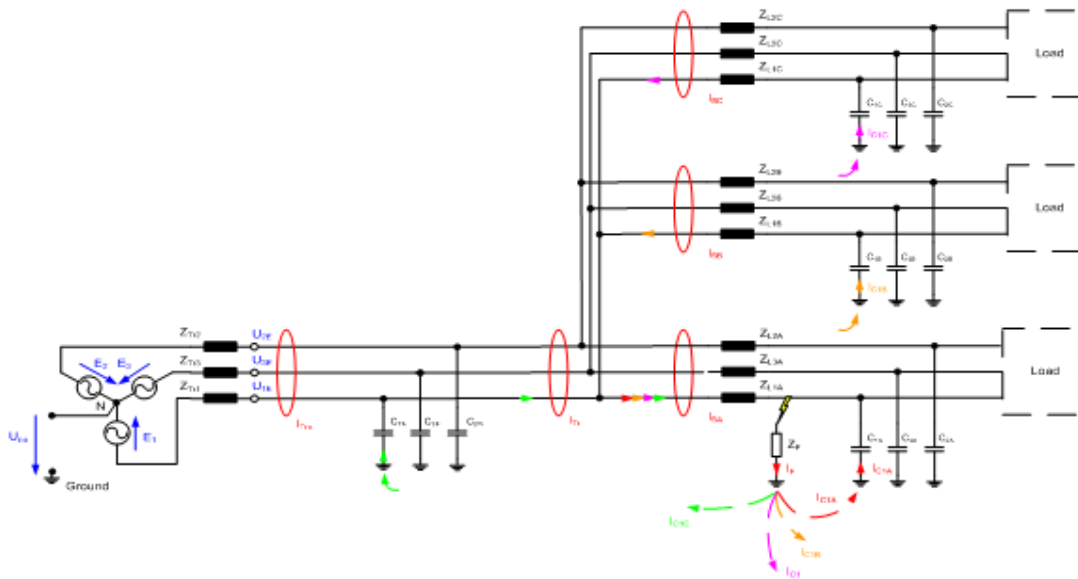


Figure 4.1. Discharge of the faulty overhead line

4.1.1 Discharge of the faulty overhead line

The lines can be considered as a distributed lattice network, consisting of a complex serial impedance Z_{LXX} and a line to ground capacitance C_{XX} . The greatest probability for the first ignition is near the maximum of the line to ground voltage V_{1G} . At this time the line has about the maximum charge. The discharge of the lattice network of line 1 will start at the fault location and will propagate as a wave in both directions to the ends of line 1. The supply transformer as well as the distribution transformers at the loads can be considered as high ohmic terminations of the line. The extension of the propagation of the wave to the two healthy feeders is blocked. Also, the influence of an existing Petersen Coil is blocked. Moreover, a reflection of the waves occurs at the end of the line respectively at every change of the image impedance of the line, for example at the substation or at a

splitting point from one line in two or more lines. These reflections can be detected in form of oscillations at a high frequency in the zero sequence current and voltage.

Important parameters for the behavior of the discharge are:

- Capacity of line 1 to ground.
- Charge of the line to ground capacity before the start of the first ignition.
- Serial line impedance Z_L of line 1 in the faulty feeder and in the healthy feeders.
- Impedance Z_F at the fault location, including the grounding resistance.

The lines of phase 1 of the healthy feeders can be considered as a parallel connection of these lines, which results in a lower impedance of the equivalent serial impedance and a higher equivalent line to ground capacity of the healthy feeders. The oscillation frequency essentially depends on the serial impedance and the line to ground capacity which is, in a first approximation, proportional to the length of the line. The frequency is higher for short networks and is lower for large networks. Usually, the oscillation frequency is above 10 kHz.

4.1.2 Charge of the two healthy overhead lines

As a result of the discharge of the faulty line the triangle of the voltages is destroyed and the voltage V_{1G} is more or less zero, as it could be appreciated in the next figure.

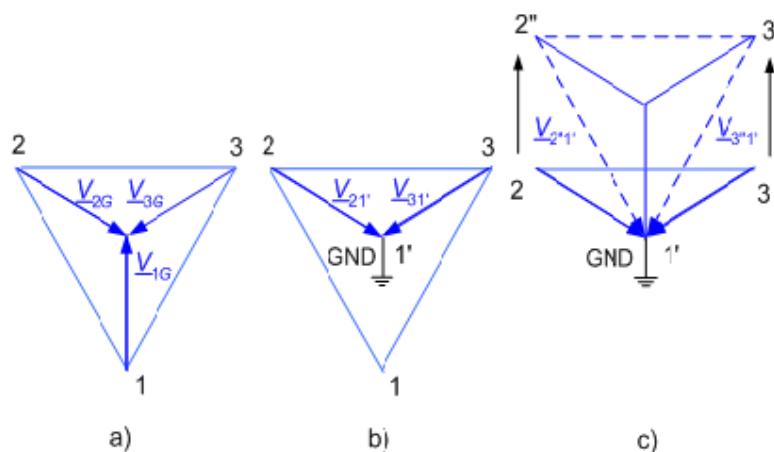


Figure 4.2. Change of the voltages during the charging process

Because the supply transformer is still delivering a symmetrical three phase system, the two healthy lines will be charged to the line to line voltage (Figure 4.2).

In the Figure 4-3 charging process for the network with three feeders is shown in detail.

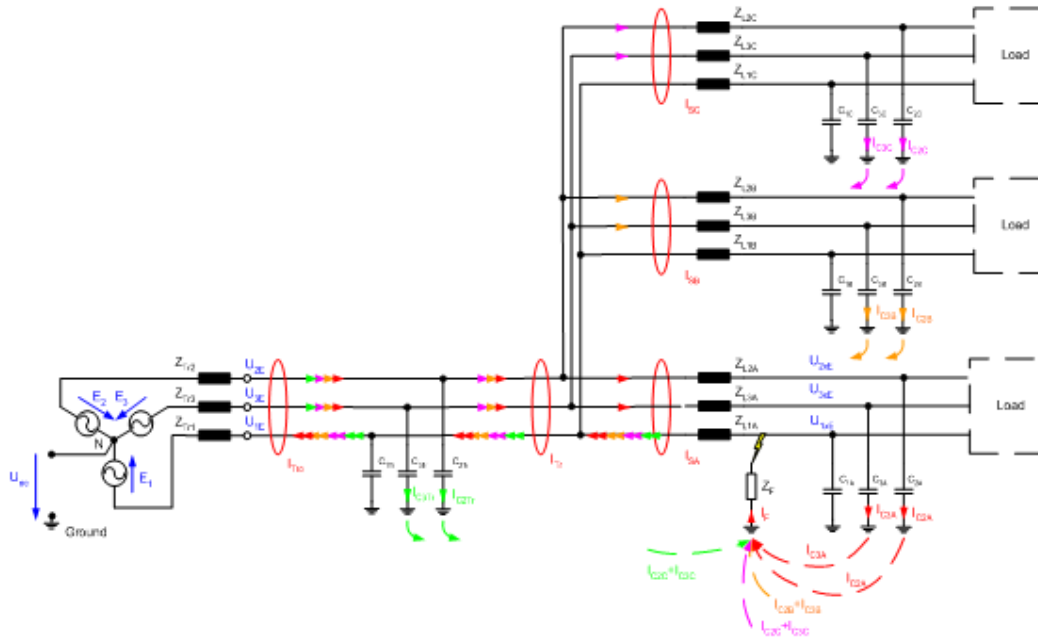


Figure 4.3. Charging of the two healthy lines over the earth

Important parameters for the behavior of the charging are:

- Capacity of line 2 and line 3 to the ground.
- Charge of the line to ground capacities before the start of the first ignition.
- Charge voltage V_{21} and V_{31} .
- Leakage inductance of the supply transformer.
- Serial line impedance Z_L of the lines.
- Impedance Z_F at the fault location, including the grounding resistance.

The distribution transformers respectively the loads are comparatively high ohmic and can be neglected in the first approximation. The resistive load results in an additional damping of the charge oscillations. If the distribution transformer has no load on the secondary side only the very high ohmic magnetizing inductance takes effect.

The essential remaining inductive components for the description of the charge oscillations are the relative low ohmic leakage inductance of the supply transformer and, for earth faults which are far away, the inductance from the point of the supply transformer to the fault location.

The influence of the Petersen Coil can be ignored, as the impedance of the Petersen Coil is much higher than the leakage inductance of the transformer.

From the last figure, the following conclusion can be made:

- Two capacitive charging currents flow into a healthy feeder. These charging currents can be measured as zero sequence currents. The amount of this zero sequence current is proportional to the line to ground capacity of this feeder.
- All the capacitive charging currents of the healthy feeders (B and C) have to flow over the fault location.
- The charging currents of the faulty feeder (A) flow over the fault location and back to the supplying transformer in line 1. As a result, these currents cannot be measured in the zero sequence system. The sum of these four currents is zero.
- The zero sequence current of the faulty feeder is the sum of all charging currents of the healthy feeders but with inverse direction. Instead of a capacitive charging current there is an inductive charging current.
- In a compensated network a superposition of the current through the Petersen Coil takes place. The effect of this current is small at the beginning of the ignition.

4.1.3 Stationary state of the earth fault

For the explanation of the stationary state also the previous figure can be used. For an isolated network the whole capacitive current of all feeders flows over the fault location. The relays of the healthy feeders measure a capacitive zero sequence current and the relay in the faulty feeder measures an inductive zero sequence current. In the stationary state, the size of this inductive current is, like in the previous section, the sum of the currents in the healthy lines in the back of the relay.

For compensated networks the situation is changed. In this case, the current through the Petersen Coil superposes and reduces the capacitive current over the fault location. In a well tuned network the capacitive current over the fault location is completely compensated. From Figure 4.3, it can be seen that in this case the relay in the faulty feeder measures also a capacitive zero sequence current, as well as the relays in the healthy feeders. Therefore, in compensated networks the inductive character of the zero sequence current is no longer an indication of a faulty line.

Using a Petersen Coil, the current over the fault location can be reduced to the small watt metric part, which is usually in the range of 2 to 3 per cent of the whole capacitive line to ground current of the network.

4.1.4 Approach of the qu method

To avoid the disadvantages of conventional transient relays a new method was developed. In the section “Charge of the two healthy overhead lines” it was shown that the two healthy lines were charge to the line to line voltage by the earth fault. This charging can be seen in the zero sequence system.

The following considerations are based on the transient definition of the zero sequence system according to the space vector theory.

For example, for the healthy feeder B of our sample network Figure 4-3 the charging can be described with the next equation

$$u_0(t) = u_0(t_0) + \frac{1}{C_{eqB}} \int_0^t i_{0B}(\tau) d\tau \quad 4.1$$

$$u_0(t) = u_0(t_0) + \frac{q_S(t)}{C_{eqB}} \quad 4.2$$

Now t_0 can be chosen that $u_0(t_0) = 0$.

$$u_0(t) = \frac{q_S(t)}{C_{eqB}} \quad 4.3$$

The new digital relays use signal processors having enough memory for large ring buffers and a sampling rate of 10kHz or higher. These features enable the relay to use even past measurement data for the calculation.

Depending on the situation, it is possible to go back to one of the zero crossings of u_0 in the past and to start the integration of the zero sequence current i_0 from this chosen point up to the actual trigger point. The result of the integrations shows that the curve of the integral of i_0 differs from the curve of u_0 only by the factor C_{eqB} , which is the equivalent zero sequence capacitance of the feeder B. the integration of i_0 represents the actual charge q_0 on the feeder.

Drawing an diagram of this relation, with the integral of i_0 on the ordinate and the zero sequence voltage u_0 on the abscissa results in a straight line with the gradient C_{eqB} . Subsequently, this diagram will be referred to as QU diagram.

In the case of a faulty feeder this relation is no more valid. The sum of the charging currents of all healthy feeders flows out of the faulty feeder. The result of the integration of the zero sequence current i_0 is no longer proportional to the zero sequence voltage.

This behaviour is shown in the next Figure for the two healthy feeders B and C and the faulty feeder A.

The integration of i_0 over a larger range makes it possible to detect also high ohmic earth faults up to some KOhm. In this case the integration has to start at a zero crossing of u_0 some periods in the past.

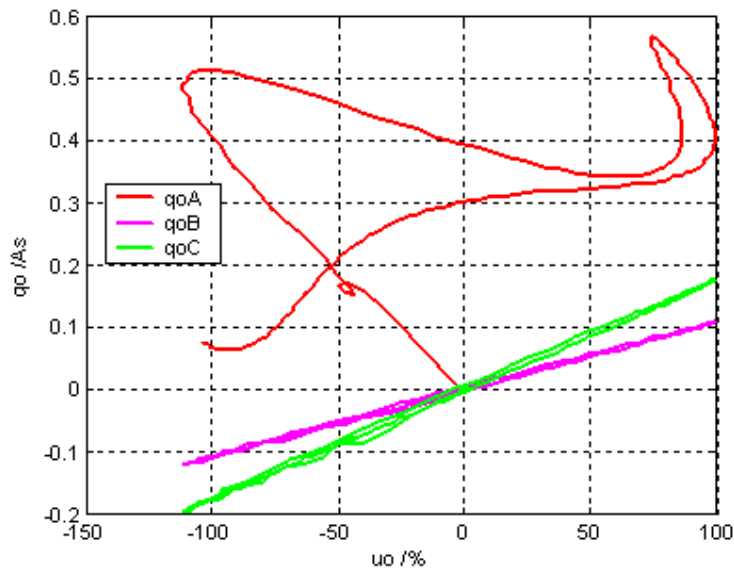


Figure 4.4. qu diagram of a low ohmic earth fault

The next figure shows the QU diagram for an earth fault with a fault impedance of 2000 Ohm.

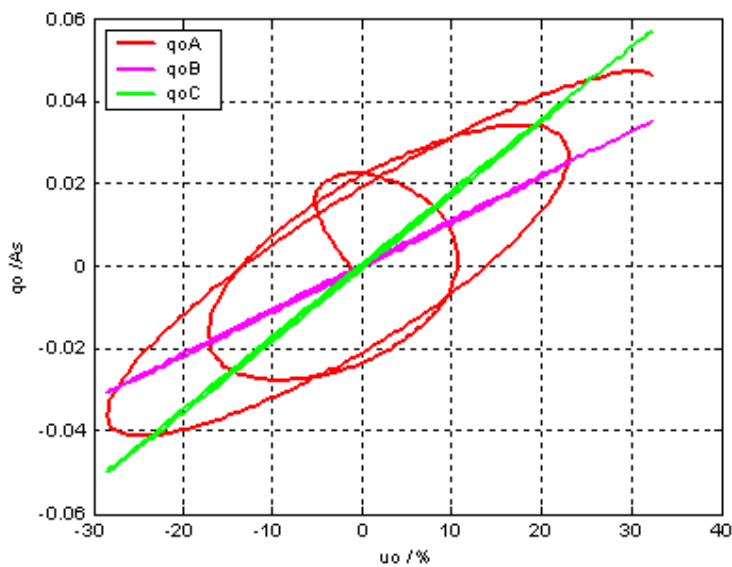


Figure 4.5. qu diagram of a high ohmic fault

Therefore, the task for detecting a transient earth fault can be solved by the decision whether the curve in the QU diagram is a straight line or not. It should be noticed that on-line versions of the least squares algorithm and pattern recognition algorithms should be implemented in the relay in order to improve the computational efficiency.

The advantages of the qu method are:

- Simple evaluation.
- No high speed sample rate is necessary. A sample rate of about 2 kHz is sufficient.
- Influence of the discharge is reduced due to the integration of i_0 .
- The integration and evaluation can be done over a half period.
- The integration of i_0 over a larger range before the trigger point enables the detection also of high ohmic earth faults up to some kOhm.
- On line versions of the least squares algorithm [21] and pattern recognition algorithms improve the computational efficiency.

On the other hand, the drawbacks of this method are:

- Sensitive to analog digital converter saturations, as the straight line is modified to a curve.
- Sensitive to not negligible phase splitting.
- Sensitive to crosstalk from parallel systems.

The first disadvantage is only relevant in case of integration over the complete half period of u_0 and in combination with testing of the feature “straight line” of healthy lines.

The sensitivity against phase splitting is a general problem of all relays

Phase splitting is the situation when two feeders supply a common load. Using the next figure the reason of phase splitting in a healthy meshed network will be explained.

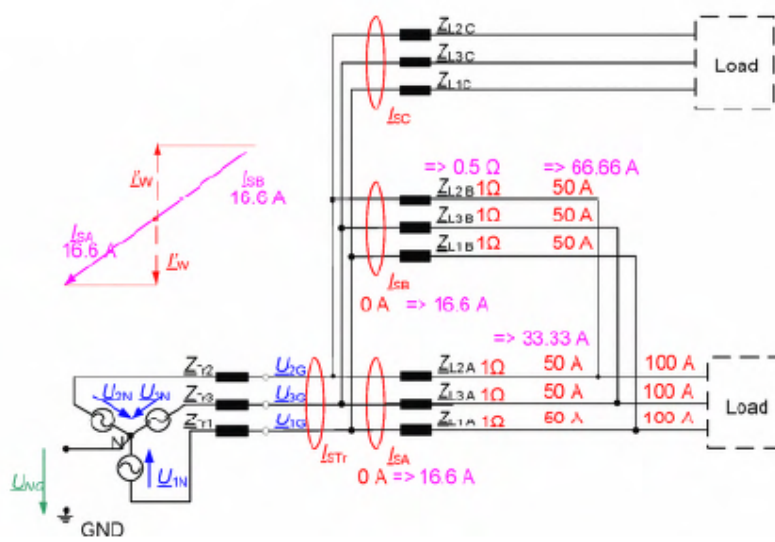


Figure 4.6. Phase splitting in the healthy network

In a symmetrical situation the load current in each phase will be splitted equally between the feeders A and B. In this situation the measured sum current ($I_S = 3I_0$) at the substation will be zero. Due to unbalances in the serial impedances of the lines the distribution of the load current will change. In the example the current in phase 2 or b is changing form 50 A to 33.3 A. respectively to 66.6 A

Now the sum currents of the feeders in the substation are no longer zero. In our example the sum current increases up to 16.6 A and the directions in the two feeders are opposite.

We can find this behaviour in any loop, in parallel lines and in meshed networks.

The size of the phase splitting current depends on:

- Load current.
- Pint of load on the loop.
- Physical arrangement of the asymmetry of the serial impedances [22].
- Number of meshes.

The asymmetry of a line may be caused for example by the kind of laying the cables, as shown in the next figure. If the cables are laid in a triangle, the mutual coupling of the three phases and therefore the serial impedance is obviously the same.

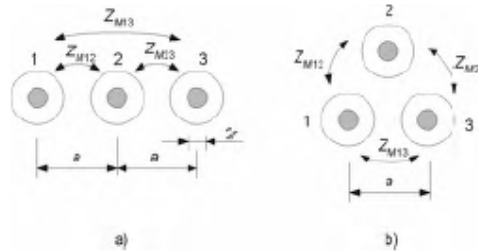


Figure 4.7. a) Single conductor cables in parallel b) Single conductor cables in triangle

A similar situation can be found for overhead lines where an improvement can be made, by transposing the phases.

One possible way to compensate this influence in loops is to measure the currents in all feeders and to add the currents of the feeders, which are switched to a loop. But this version needs a very high number of current measurements and, in addition, always the actual information, which feeders are switched to a loop. The requirements to such a SCADA system would be enormous.

Crosstalk from parallel systems

Systems switched to a loop are also very sensitive to the magnetic coupling of galvanic isolated parallel systems.

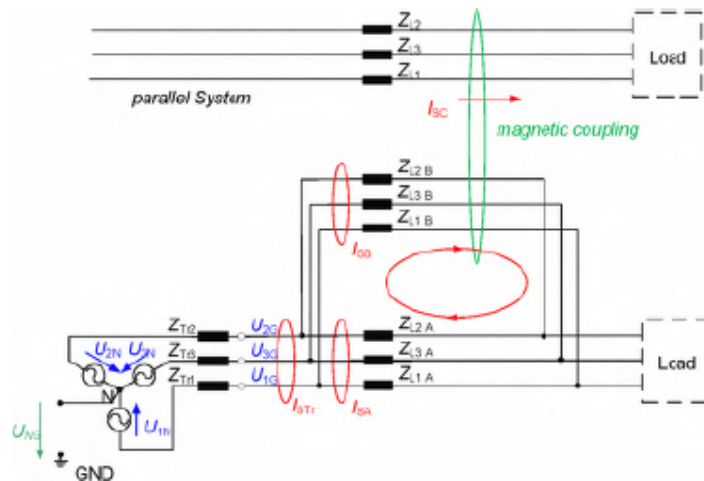


Figure 4.8. Magnetic coupling of parallel systems

The influence of the parallel system may be negligible under normal operation, due to the small distances between the three phases. But in case of an earth fault in the parallel system, the currents through the three wires are no more symmetrical, also in healthy feeders (Figure 4.8). The asymmetric loading currents can be in the range of 100 A. therefore the magnetic coupling must be taken into account.

A worse situation arises in case of a cross country fault in the parallel system. Also, a phase splitting in the parallel system can be reason for a crosstalk.

Chapter 5

5 PSCAD MODEL

The network consists of a bus bar with three feeders and a station transformer (Østeras). The nominal voltage is 22 kV and the only connection to ground apart from the capacitances to ground is via the neutral of the station transformer. An arc suppression coil and a parallel resistance could be connected between the neutral and ground. One feeder (Sparbu) is represented by a 5km length of overhead line and without any load. The single phase to ground fault is applied to this feeder. The two other feeders (Henning and Sandvollan) consisted mainly of overhead lines and short length cables.

Most of the information in this section was based on [23]

Measurements were taken in the three bus bar voltages to ground and the zero sequence current of the three feeders. The current of the Petersen Coil and the parallel resistance were measured during the simulations and the fault current was measured as well.

When the single phase fault was applied, the following parameters were varied:

- Degree of compensation: 0, 80 and 100%
- Parallel resistance connected or disconnected
- Fault resistance

The measured signals were recorded within 1 s. of simulation. The steady state before the fault covers the interval from 0s until 0.6s, and the transient and steady state due to the fault is taken in the interval from 0.6s until 1s.

5.1 Transmission line representation

For the sequence networks to correctly represent a power system, the power system components must be correctly modeled in the networks. The necessary complexity of the components models depends on what kind of analysis the networks shall be used for. Within this work, the networks shall be mainly used for fundamental frequency analysis. Nevertheless, a good transient response representation of the system will be required by the location and detection method shown in this document.

In this work, the overhead lines would be represented by a distributed parameter formulation, in order to fulfill the requirements of the charge voltage method and give a more real representation to the system.

The distribution network in reality is composed by hundreds of different kind of overhead lines and cables. Nevertheless, the length data of the different type of overhead lines was given by SINTEF and the overhead line representation was successfully modeled. On the other hand, the cables due to their short length in the system were represented by ground capacitances, whose values were calibrated based on measurements in the isolated neutral system.

5.1.1 Overhead lines

The distributed parameter formulation, which is excellent for simulation evaluation according to [24], was taken over in the overhead line model.

The T-Line configuration was chosen to represent all the overhead lines in the system as it can be seen in the next figure. Within the T-Line configuration, there are several different options for the desired representation of the line.

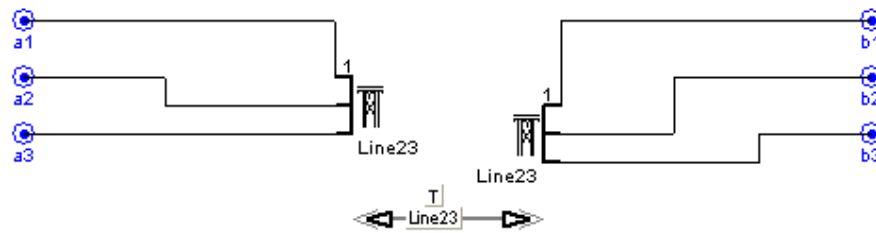


Figure 5.1. T-Line Configuration

The Frequency Dependent Model was selected as line model within the configuration. Basically a distributed RLC traveling wave model, which incorporates the frequency dependence of all parameters, the model represents the frequency dependence of internal transformation matrices. It is worth to mention, that the model uses curve fitting to duplicate the response of the line. It is the most advanced time domain model available as it represents the full frequency dependence of all line parameters (including the effect of a frequency dependent transform).

The line model used is useful for studies wherever the transient or harmonic behavior of the line is important, as in the system presented in this document, where the fault location and detection method requires the transient behavior of the system when a high fault resistance.

In the model taken, the topology used was the same for all the overhead lines and is shown in the Figure 5.2. The parameters needed for the right representation were:

- Conductor Geometric Mean radio.
- Conductor DC Resistance.
- Height of all conductors.
- Horizontal spacing.
- Shunt conductance (this values was taken as zero).

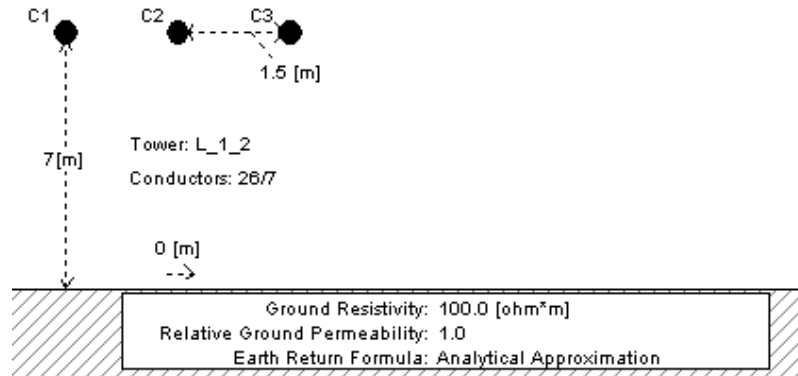


Figure 5.2. Overhead Line Topology

5.1.2 Cables

The distributed zero sequence parameters of cables differ substantially from those of overhead lines. Both series impedance and shunt capacitance is considered proportional to cable length. The series impedance of short cable is therefore small in relation to the shunt impedance. If the cables are short enough, the series impedance is negligible and the shunt capacitance alone makes up the representation of the cables. Since length of the cable feeders in conventional distribution systems is limited to a few kilometers, it has become common practice to neglect cable feeder series impedance in distribution system analysis [10], [11] and [25]

Taking the previous reference, the cables were represented by ground capacitances, whose values were calibrated based on measurement in the isolated neutral system, the capacitors per feeder were modeled completely balanced.

5.1.3 Load Transformers

The main transformer station is supplying the three feeders Sandvollan, Henning and Sparbu, that would be described further in this work. As it was mentioned previously, the Sparbu feeder (faulty feeder) was disconnected, thus, the feeder is not loaded.

In the reality, Henning feeder and Sandvollan feeder are loaded with 57 and 104 respectively, in the model represented in PSCAD, it was assumed concentrated at the secondary side of a transformer, which is Y coupled in the primary and Δ coupled in the secondary.

The load itself was represented as a fixed load, which models the load characteristic as a function of voltage magnitude and frequency. The active Power and reactive Power are input parameters in this model, as well as the phase to ground rated voltage.

5.1.4 Feeder Conductance

With the purpose to have a PSCAD model closer to the real the network, the feeder conductance could be calculated from data exposed in [7]. The representation was taken as phase to ground parallel resistance, which was connected just after the main transformer and before the feeders connection, the resistance value is 45 k Ω for each phase.

5.2 Substation

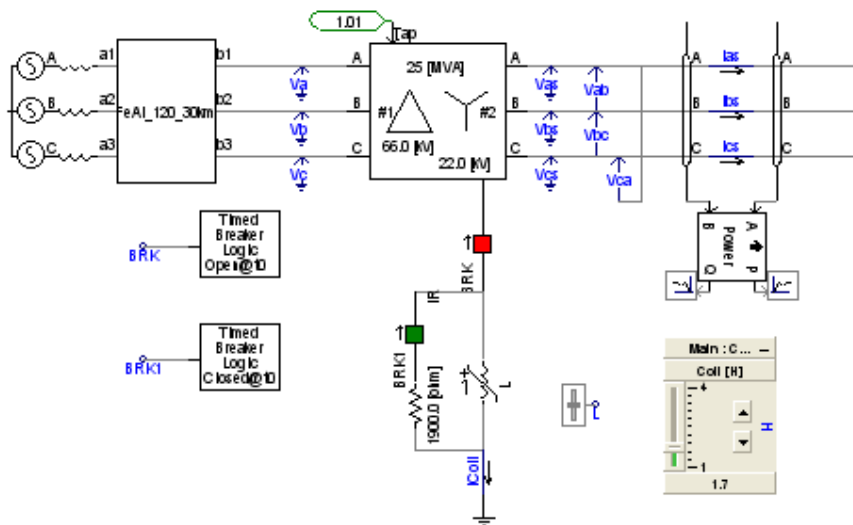


Figure 5.3. Østeras substation Representation

In Figure 5.3, it is found the substation representation used in the PSCAD model. Firstly, a three phase voltage source with magnitude of 66 kVrms with leakage inductance of 10 mH is represented as the feeding system.

A transmission overhead line follows the three phase voltage source until a 25 MVA main transformer, which represents the Østeras substation itself. Throughout the transformer, which is Δ coupled in the primary and Y coupled in the secondary, different grounding systems were implemented in order to perform the simulations concerning to each case. From Østeras substation, there are three feeders; Henning, Sparbu and Sandvollan.

In this part of the model, the phase to ground voltage, the phase currents after the transformer and output power were measured throughout the simulations.

5.3 Henning Feeder

The Henning feeder takes part in the model as one of the healthy feeders. In Figure 5.4, a cable representation was made throughout phase to ground capacitors and three overhead lines representations, which are modelled with three blocks with description label about the length and the type of line, inside of each of this block the line configuration previously describe would be found.

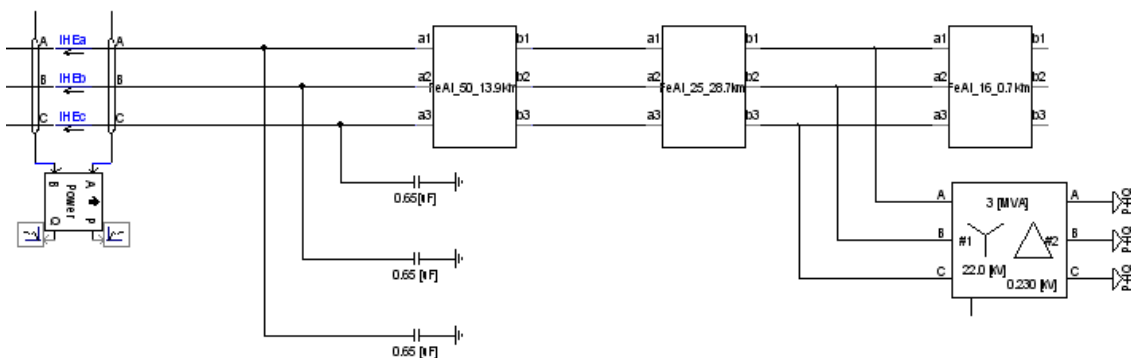


Figure 5.4. Henning Feeder representation

It was assumed concentrated load at the secondary side of the load transformer, which goes from 22 kV until 0.230 kV and has a rated power of 5 MVA. The measurements taken in this feeder are the current in each phase and the active and reactive power input into the feeder.

5.4 Sparbu feeder (FAULTY feeder)

The fault was applied in Sparbu feeder. According to the field test, the fault was 500 m, according to [7], away from Østeras substation, keeping the rest of the feeder disconnected from the substation, which was represented as the main transformer in this model.

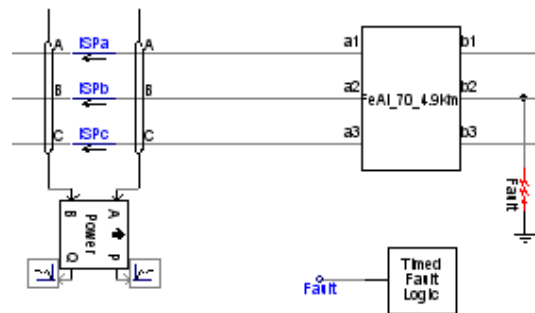


Figure 5.5. Sparbu feeder representation

The only impedance presented in the feeder was the biggest overhead line dimension registered in it. The fault takes place on the phase b of the system. The measurements taken in this section are concerning to the phase currents and the input power.

5.5 Sandvollan feeder

Figure 5.6 shows how it was modeled Sandvollan feeder, which represents the longest feeder in the system. The feeder is composed by four blocks, which represents overhead lines, and the cable modeling was taken over throughout a ground capacitor in each phase due to the short length of the cable.

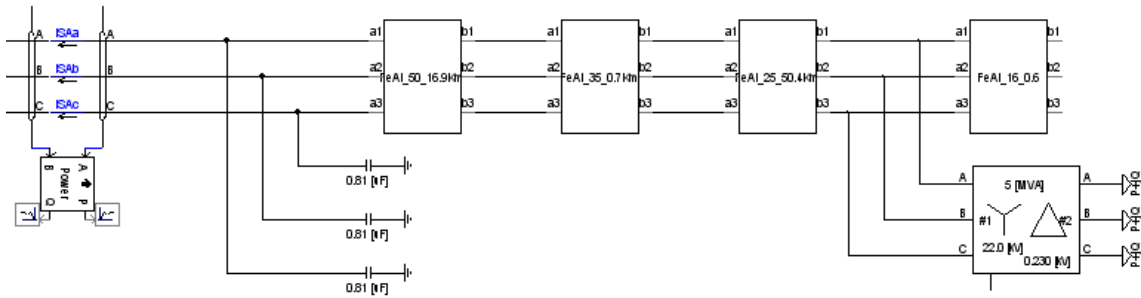


Figure 5.6. Sandvollan feeder representation

It was assumed concentrated load at the secondary side of the load transformer, which goes from 22 kV until 0.230 kV and has a rated power of 5 MVA. The measurements taken in this feeder are the current in each phase and the active and reactive power input into the feeder.

5.6 Special blocks

At present, PSCAD can represent Phasor domain quantities through the use of various meters and functions. In particular, the FFT or (On-line Frequency Scanner) shown in Figure 5.7, has the ability to output both Fourier magnitude and phase values for multiple harmonics (including DC offset), for any input signal.

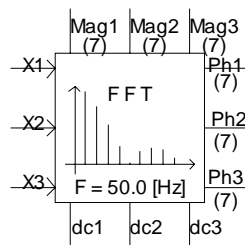


Figure 5.7. On-line Frequency Scanner (FFT)

The FFT component itself is a very powerful and important tool in the PSCAD Master Library, the matter of fact it was the great help during the development of the system described in this work. The display device will show either a single phasor or the phasors in an adjustable gauge display. Numerical values for the magnitude and phase angle are given at the footer panel of the device, as it could be seen in the next figure.

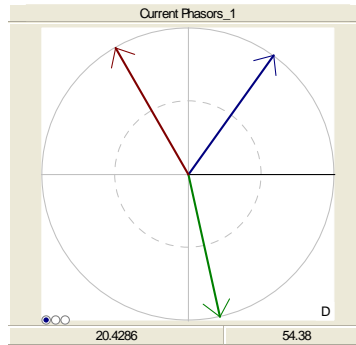


Figure 5.8. Phasor-meter

5.7 Parameter settings

All the parameters presented in this section are referred as single phase values, except from the apparent power and the winding relation of the load transformers, as well as the main transformer.

The parameters presented below were taken from [26]

Regarding the balance of the system, the cable capacitances and the fixed loads are represented totally balance. The only unbalance takes in this work, are the overhead lines, which are modeled as no ideally transposed.

5.7.1 Main transformer (Østeras)

Table 5-1. Main Transformer parameters

S [MVA]	Relation [kV/kV]	X_{cc} [PU]	R_{cc} [PU]
25	66/22	0.095	0.0043

5.7.2 Henning Feeder

Table 5-2. Overhead Lines parameters

Line type	Length [Km]	R [Ω]	X_L [Ω]	C_g [nF]
FeAl 50	13.9	5	5.22	69
FeAl 25	28.7	20.75	11.39	138
FeAl 16	0.7	0.75	0.28	3.33

Table 5-3. Cable parameters

C_g [μF]	0.65
-------------------	------

Table 5-4. Load transformer parameter

S [MVA]	Relation [kV/kV]	X_{cc} [PU]	R_{cc} [PU]
3	22/0.230	0.08	0.004

Table 5-5. Fixed Load parameters

Active Power [MW]	Reactive Power [MVar]
0.571	0.187

5.7.3 Sparbu Feeder

Table 5-6. Overhead Lines parameters

Line type	Length [Km]	R [Ω]	X_L [Ω]	C_g [nF]
FeAl 70	4.9	1.27	1.78	24.73

5.7.4 Sandvollan Feeder

Table 5-7. Overhead Lines parameters

Line type	Length [Km]	R [Ω]	X_L [Ω]	C_g [nF]
FeAl 16	0.6	0.65	0.24	83.7
FeAl 25	50.4	36.45	20	3.42
FeAL 35	0.7	0.36	0.27	243
FeAl 50	16.9	6.08	6.34	83.7

Table 5-8. Cable parameters

C_g [μF]	0.81
-------------------	------

Table 5-9. Load Transformer parameters

S [MVA]	Relation [kV/kV]	X_{cc} [PU]	R_{cc} [PU]
5	22/0.230	0.08	0.004

Table 5-10. Fixed Load parameters

Active Power [MW]	Reactive Power [MVar]
1.358	0.446

Chapter 6

6 RESULTS

The phasors were calculated from the FFT block mentioned in the previous chapter, when the studied variables reached their steady state behavior. The phasors are represented in two tables, the first is covering the RMS values of the selected variables and the second table is covering the phase angle of the phasors with the phase of the zero sequence voltage as reference.

The magnitude values of the field test, as well as the phase were taken from [7].

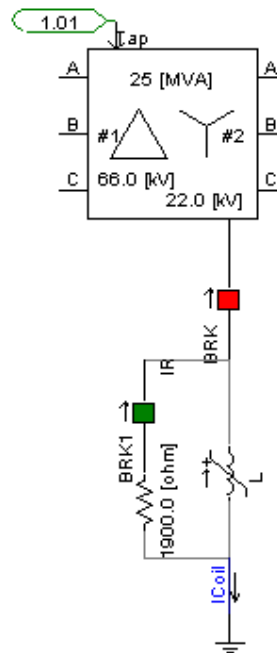


Figure 6.1. Arc Suppression coil arrangement with parallel resistance

From the previous figure, it can be shown the different conditions in which the network can be operated. Therefore, it is possible to disconnect the coil completely and to operate with or without parallel resistance.

Following, the next conditions were considered in the simulations:

- Isolated Condition
- 100% Compensation with Parallel Resistance Connection
- 80% Compensation with Parallel Resistance Connection
- 80% Compensation
- 80% Compensation with Parallel Resistance Connection with high fault resistance
- 100% Compensation with high fault resistance

The high resistance used was equivalent to 3000Ω , meanwhile in the other case, an ideal fault was implemented ($R_f = 0$).

The focus in the analysis of the results will be headed to the zero sequence currents, due to the direct relation with the fault current, which is the main subject in this work.

6.1 Isolated Condition

In this case, the Main transformer (\emptyset steras) is completely isolated, thus, the main breaker is open. During this condition, the cable representation was calibrated until getting similar results with the field test. The focus of this calibration was made in the zero sequence currents, because in these is involved the fault current. Therefore, in the next two tables can be seen, the final values gotten in this condition.

Table 6-1. Phasors Magnitude for Isolated Condition

Value Source	Simulation	Field Test
Compensation	Isolated	Isolated
$3I_{0HE}$ [A]	10.43	9.61
$3I_{0SP}$ [A]	24.46	22.29
$3I_{0SA}$ [A]	14.01	12.81
I_{Coil} [A]	-	-
U_a [kV _{rms}]	22.12	22.68
U_b [kV _{rms}]	0.1	1.69
U_c [kV _{rms}]	22.06	21.14
U_0 [kV _{rms}]	12.81	12.64
I_f [A]	24.77	-
I_{Rp} [A]	-	-

Table 6-2. Phasors Angle for Isolated Condition

Angle Shift	Simulation	Field Test
Compensation	Isolated	Isolated
$3I_{0HE}$	-90	-90.3
$3I_{0SP}$	87.93	89.35
$3I_{0SA}$	-90	-89.75
I_{Coil}	-	-
U_a	-29.63	-26.25
U_b	-24.09	-91.10
U_c	29.93	33.66
$U_0 REF$	88.37	-
I_f	-92	-

It can be seen, from the previous values, that difference between the field test numbers and the simulation ones are within an approximate error of less than ten per cent. This difference could not be less, because there is a direct relation with Petersen coil calculations, as it will be shown further on.

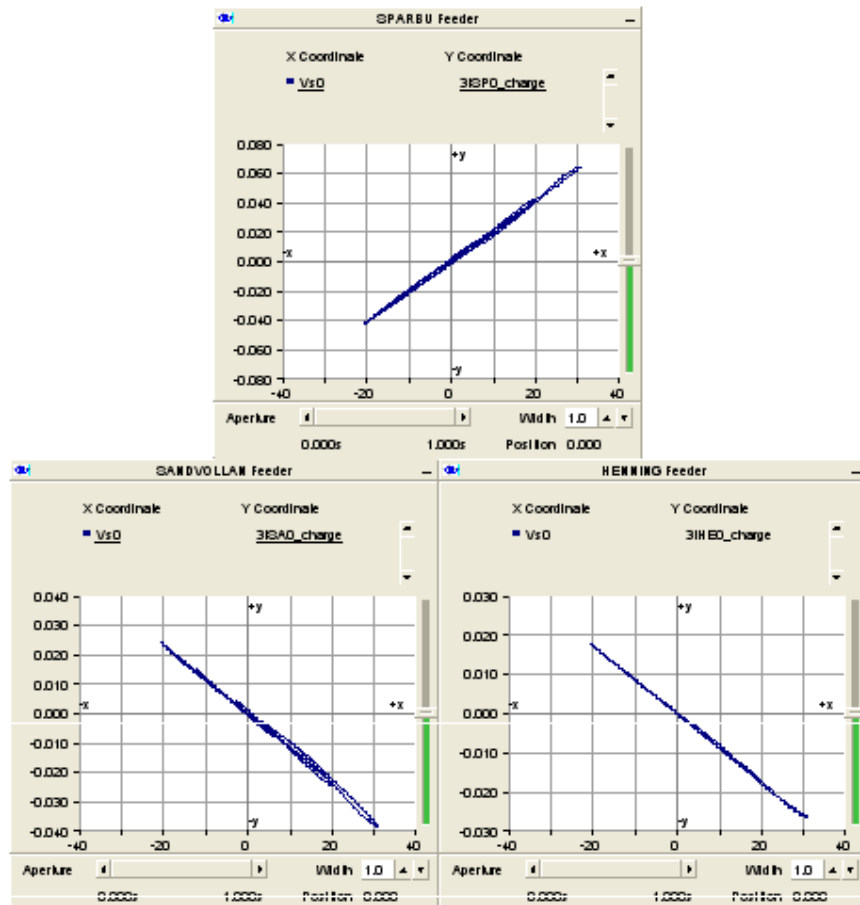


Figure 6.2. QU Diagram in Isolated System

In the Figure 6.2 is presented the charge voltage curves in an isolated system, it is noticed that the shape of the curve for the faulty feeder (Sparbu) is practically the same as for the healthy feeder except for a change in the sign, and this is due to the disconnection of the coil and parallel resistance (Isolated state) and thus, the fault current is minus the sum of the currents of the healthy feeders.

In this case, the faulty feeder cannot be identified by the shape of the charge – voltage curve; however, it can be identified based on the sign of the current.

The diagram gotten from the field test measurement exposed in [27] possesses similar behaviour with the one gotten from the simulations.

6.2 Resonance curve calculations

According to the theory exposed in this document, the resonance curve was obtained throughout the measurements of the neutral to ground voltage, or how it is called further on, zero sequence voltage, meanwhile the Petersen Coil is tuning. During the simulations, the distribution network was without faults.

The resonance curve was measured in two versions, both with and without the parallel resistance (R_p) connected, whose values is 1900 Ω . The value of the parallel resistance was taken from the measurements taken in [7].

The voltage curves presented in this work are in function of Amps (A), and it comes from the next equation.

$$I = \frac{U_{L-G}}{\omega L} \tag{6.1}$$

In the previous equation the U_{L-G} is rated rms phase to neutral voltage of the second winding of the main transformer, ω represents the angular frequency and L is the Petersen coil value at the moment of the measurement.

In the field test, measurements in under compensation was made, the grade of under compensation was only 80%. Information about under compensation and/or over compensation could not be found in the literature. Therefore, 80% under compensation was taken as the corresponded value of Petersen Coil, when the zero sequence voltage is 0.8 of U_0 in 100% compensation (Maximum Voltage of the curve).

6.2.1 Resonance curve with Parallel resistance connection

The arc suppression coil and the parallel resistance arrangement were connected to the main transformer, in the simulations, measurements of the neutral to ground voltage of the transformer were taken, when the distribution network did not present any fault. In the next table, it is found the results of the simulations.

Table 6-3. Resonance Curve data

Petersen Coil [H]	U_0 [kV_{rms}]	$U_{L-G}/\omega L$ [A_{rms}]
1.4	282	28.88
1.5	310	26.95
1.66	328	24.36
1.7	327	23.78
1.8	318	22.46
1.9	303	21.28
2.15	264	18.81

The Figure 6.3 shows the Resonance Curve from the previous table, the shape of the curve is as expected due to the connection of the parallel resistance, which decreases the maximum voltage when the system is 100% compensated. Therefore, from the figure it can be extracted the following information.

- 100% Compensation, when Petersen Coil is 1.66 H.
- 80% under Compensation, when Petersen Coil is 2.15 H.

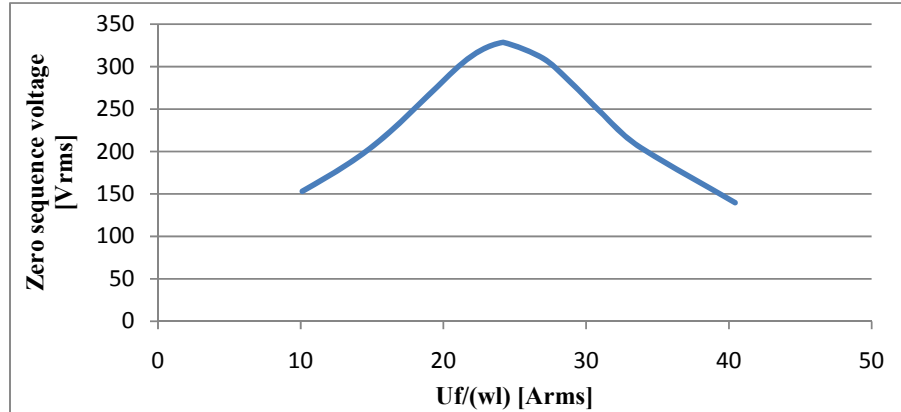


Figure 6.3. Resonance Curve with parallel resistance connection

6.2.2 Resonance Curve without Parallel Resistance Connection

The breaker of the parallel resistance was opened during these simulations, leaving the arc suppression coil as the only connection between the neutral of the main transformer and ground. In the next table, it is shown a representative sample of the measurements taken for the resonance curve calculations.

Table 6-4. Resonance Curve Data

Petersen Coil [H]	U_0 [kV_{rms}]	$U_{L-G}/\omega L$ [A_{rms}]
1.4	539	28.88
1.5	909	26.95
1.66	2842	24.36
1.7	2353	23.78
1.706	2248	23.70
1.8	1178	22.46
1.9	770	21.28

The Figure 6.4 shows the Resonance Curve of the distribution network without the parallel resistance connection. It is seen from both resonance curves, that the zero sequence voltage is rather high at 100% and 80% compensation without the parallel resistor. Thus, the next values can be gotten from the curve:

- 100% Compensation, when Petersen Coil is 1.66 H.
- 80% under Compensation, when Petersen Coil is 1.706 H.

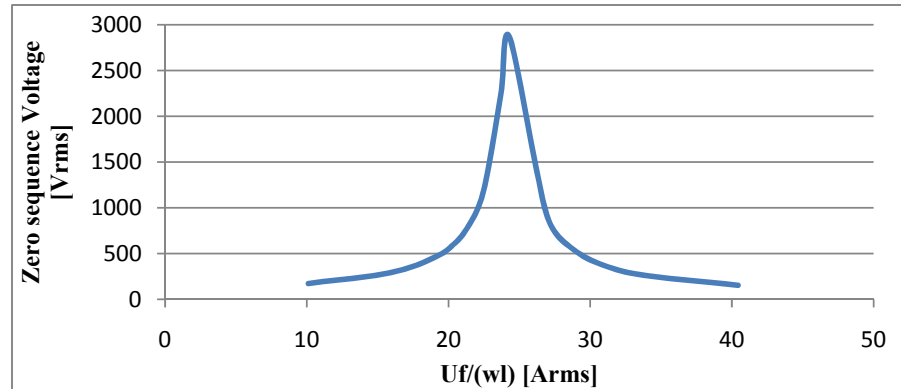


Figure 6.4. Resonance Curve without parallel resistance connection

6.3 100% Compensation with Parallel Resistance Connection

The main breaker and the parallel resistance breaker were closed during the simulations in this condition. The steady state results are shown in the next tables.

Table 6-5. Phasors Magnitude with Parallel Resistance Connection

Value Source	Simulation	Field Test
Compensation	100%+ R_p	100%+ R_p
$3I_{OHE}$ [A]	10.31	9.33
$3I_{OSP}$ [A]	7.5	7.48
$3I_{OSA}$ [A]	13.85	12.29
I_{Coil} [A]	25.16	26.85
U_a [kV _{rms}]	21.97	21.48
U_b [kV _{rms}]	0.03	0.58
U_c [kV _{rms}]	21.92	21.55
U_0 [kV _{rms}]	12.67	12.15
I_f [A]	7.5	-
I_{Rp} [A]	6.66	-

It could be seen from the presented results, that the behavior in these two different scenarios are quite similar. It is convenient to mention that the Petersen Coil used in the simulation was 1.66 H, which is the same value that has the maximum zero sequence voltage in the resonance curves.

Table 6-6. Phasors Angle for 100% Compensation with Parallel Resistance Connection

Angle Shift	Simulation	Field Test
Compensation	100%+ R_p	100%+ R_p
$3I_{0HE}$	-90	-90
$3I_{0SP}$	-0.8	1.85
$3I_{0SA}$	-90	-90
I_{Coil}	-74.67	-81.27
U_a	-29.87	-30.6
U_b	-110.8	-169.91
U_c	30.1	30.6
$U_0 REF$	88.4	-
I_f	-178.4	-

The shape of the charge voltage relation is significantly different for the faulty feeder. Therefore, the faulty feeder can be easily identified throughout the next figure.

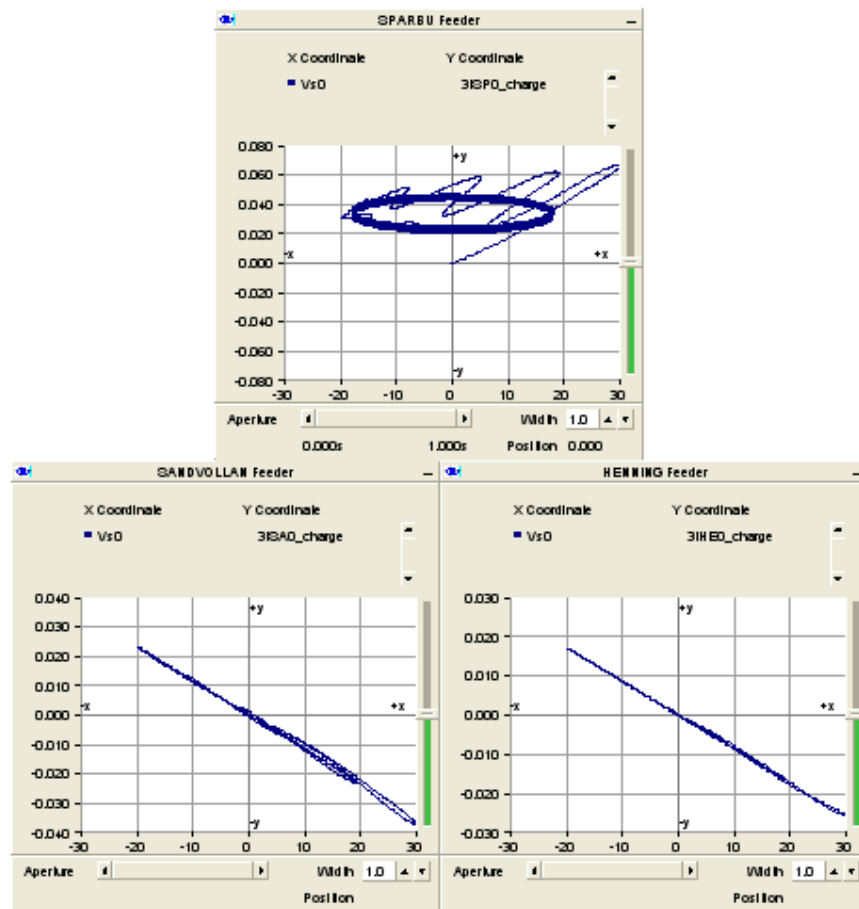


Figure 6.5. QU Diagram in 100% Compensation and Parallel Resistance Connection

6.4 80% Compensation with Parallel Resistance Connection

During this condition, the parallel resistance was connected and the Petersen Coil had a value of 80% under compensation taken from the Resonance Curve with parallel resistance connection, therefore, the coil took a value of 2.15 H during this condition.

Table 6-7. Phasors Magnitude in 80% Compensation with Parallel Resistance Connection

Value Source	Simulation	Field Test
Compensation	80%+ R_p	80%+ R_p
$3I_{0HE}$ [A]	10.34	9.39
$3I_{0SP}$ [A]	9.28	8.57
$3I_{0SA}$ [A]	13.88	12.24
I_{Coil} [A]	19.93	22.42
U_a [kV _{rms}]	22.01	21.62
U_b [kV _{rms}]	0.04	0.67
U_c [kV _{rms}]	21.94	21.42
U_0 [kV _{rms}]	12.7	12.16
I_f [A]	9.46	-
I_{Rp} [A]	6.67	-

Table 6-8. Phasors Angle in 80% Compensation with Parallel Resistance Connection

Angle Shift	Simulation	Field Test
Compensation	80%+ R_p	80%+ R_p
$3I_{0HE}$	-90	-90.31
$3I_{0SP}$	35.85	30.6
$3I_{0SA}$	-90	-89.9
I_{Coil}	-70.44	-76.82
U_a	-29.8	-29.9
U_b	-74.93	-149.57
U_c	30	31.26
U_0 REF	88.35	-
I_f	-142.6	-

After having the values from the previous two tables, it could be seen that the similarities between the simulation made and the field test are still consistent.

The Figure 6.6 shows the charge voltage curve based on 1s interval. The faulty feeder is easy to identify due to the transient part of the current.

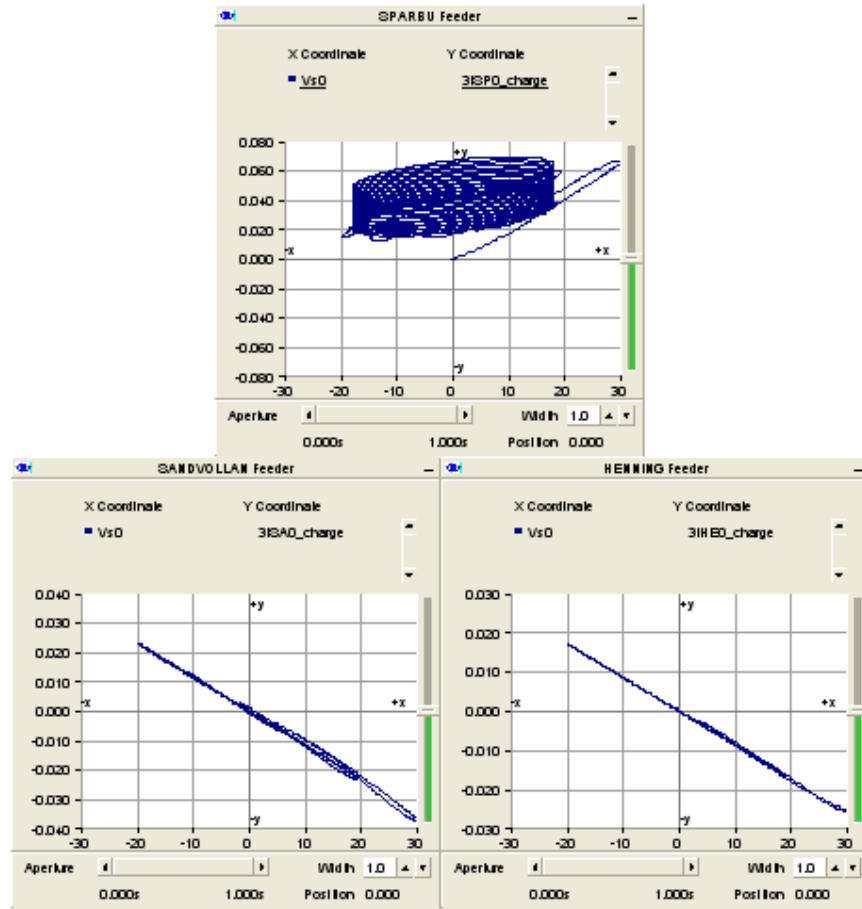


Figure 6.6. QU Diagram in 80% Compensation with Parallel Resistance Connection

6.5 80% Compensation

Table 6-9. Phasors Magnitude in 80% Compensation System

Value Source	Simulation	Field Test
Compensation	80%	80%
$3I_{0HE}$ [A]	10.34	9.77
$3I_{0SP}$ [A]	5.53	5.04
$3I_{0SA}$ [A]	13.9	12.72

$I_{Coil} [A]$	18.8	20.72
$U_a [kV_{rms}]$	22	22.05
$U_b [kV_{rms}]$	0.023	0.42
$U_c [kV_{rms}]$	21.97	21.83
$U_0 [kV_{rms}]$	12.71	12.66
$I_f [A]$	5.8	-
$I_{Rp} [A]$	-	-

Table 6-10. Phasors Angles in 80% Compensation System

Angle Shift	Simulation	Field Test
Compensation	80%	80%
$3I_{OHE}$	-90	-90
$3I_{OSP}$	81.08	80.41
$3I_{OSA}$	-90	-89
I_{Coil}	-89.9	-97.68
U_a	-29.86	-29
U_b	-30.86	-98
U_c	30	33
$U_0 REF$	88.52	-
I_f	-98.5	-

The parallel resistance was not set up in this condition, the main breaker was closed, having in this case the Petersen Coil connected between the main transformer neutral point and ground. The value of the coil is the same as the previous case (Coil = 2.15 H).

The consistence between the simulation and the field tests quantities remains.

In this condition, the faulty feeder is easy to identify due to the transient part of the current. Mean while the healthy feeder posses the expected shape.

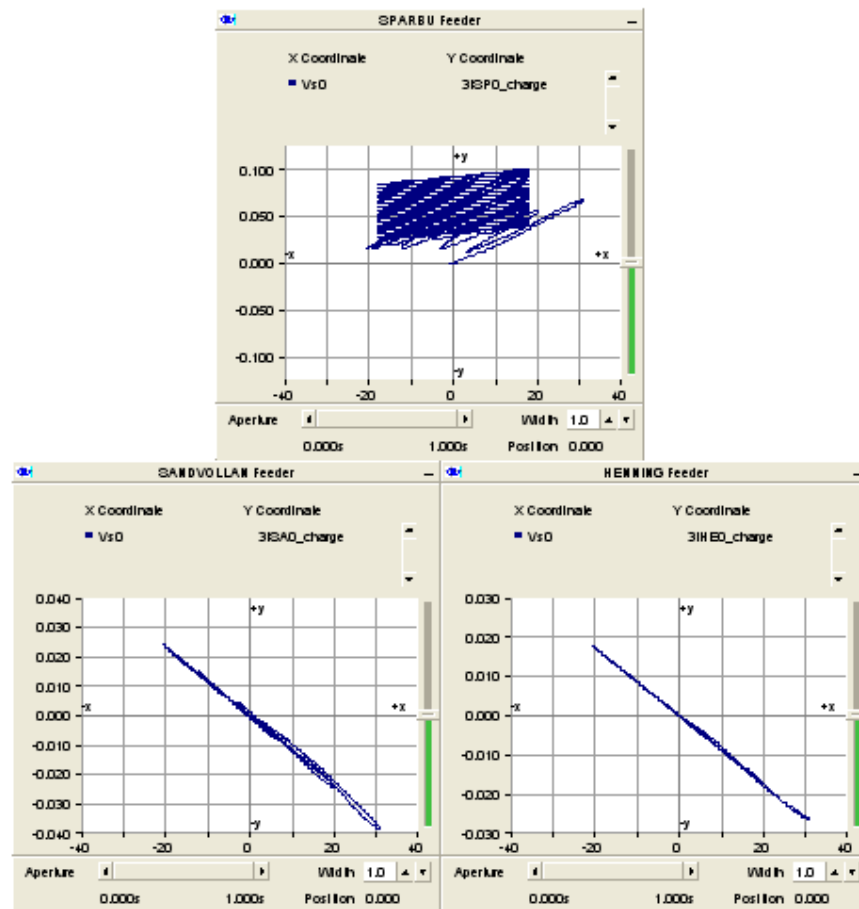


Figure 6.7. QU Diagram in 80% Compensation system

6.6 80% Compensation with Parallel Resistance and High fault Resistance

The current case was the only one among the presented simulations, in which was used the 80% under compensation coming from the resonance curve without the parallel resistance connection. The Peterson coil, which had a value of 1.706 H, was connected between the neutral of the main transformer and ground, as well as the parallel resistance.

In this condition, the fault resistance had a value of 3000 Ω . The effect of the latest can be easily appreciated in the results given in the simulation, as well as in the field test.

Table 6-11. Phasors Magnitud in 80% Compensation with Parallel Resistance and High Fault Resistance

Value Source	Simulation	Field Test
Compensation	80%+ R_p	80%+ R_p
$3I_{0HE}$ [A]	3.74	3.32
$3I_{0SP}$ [A]	2.69	2.64
$3I_{0SA}$ [A]	5.09	4.68
I_{Coil} [A]	8.85	9.49
U_a [kV _{rms}]	15.8	15.63
U_b [kV _{rms}]	8.14	8.28
U_c [kV _{rms}]	15.11	14.82
U_0 [kV _{rms}]	4.57	4.39
I_f [A]	2.71	-
I_{Rp} [A]	2.4	-

Table 6-12. Phasors Angle in 80% Compensation with Parallel Resistance and High Fault Resistance

Angle Shift	Simulation	Field Test
Compensation	80%+ R_p	80%+ R_p
$3I_{0HE}$	-89.9	-90.98
$3I_{0SP}$	6.7	7.81
$3I_{0SA}$	-89.8	-89.28
I_{Coil}	-74.26	-85.71
U_a	-40.43	-39.16
U_b	-170.8	-167.53
U_c	50	51.86
U_{0REF}	82.62	-
I_f	-170.8	-

It can be seen from the previous two tables, that the results between the simulation and the field test are consistent, and it can be noticed how the angle of the faulty feeder (Sparbu) changed due to the value of the Petersen Coil.

In the current case, the high fault resistance has a really strong influence on the fault current, as it is noticed from the tables. The transients in voltage and in current have a much shorter influence than in the previous cases, that the fault resistance was zero.

The steady state of the faulty feeder current is approximately in phase with the zero sequence voltage due to the relatively high fault resistance. The charge voltage curve of the faulty feeder is therefore approaching an ellipse as can be observed in the next figure. It is anyhow clear that the shape of the faulty feeder is significantly different from the ones for the healthy feeders.

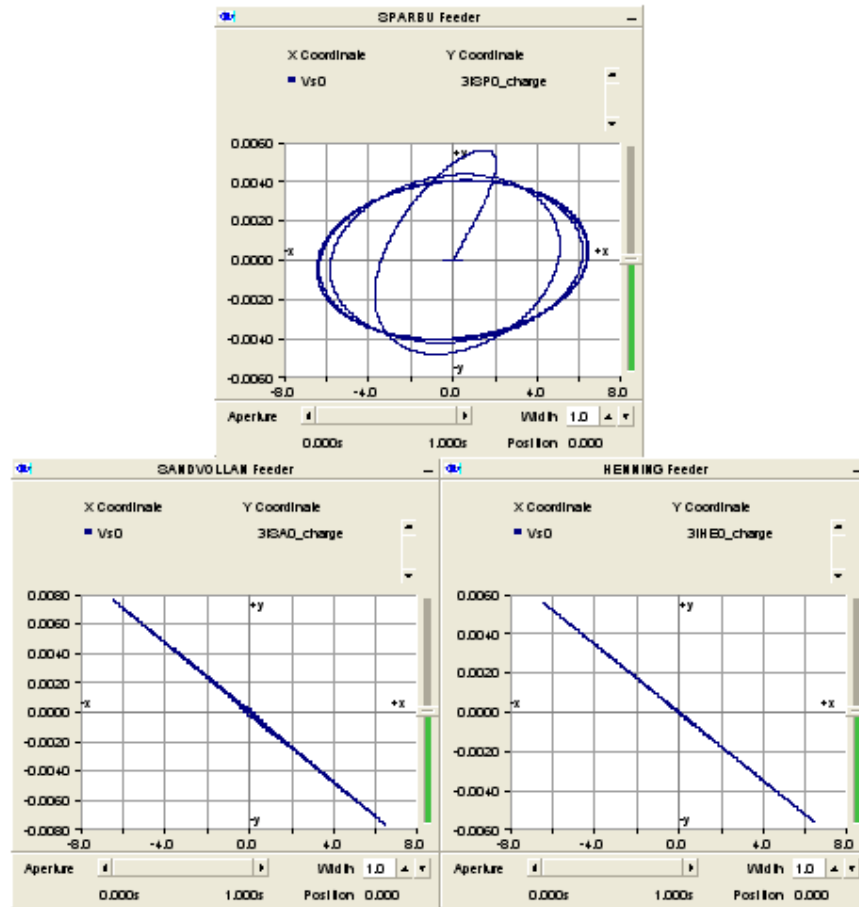


Figure 6.8. QU Diagram in 80% Compensation with Parallel Resistance Connection and high fault resistance

6.7 100% Compensation without Parallel Resistance Connection and High Fault Resistance

The current case was chosen in order to test the proposed method presented in this document. Therefore, the compensation was taken until 100%, having a Petersen Coil Value of 1.706 H and the parallel resistance was disconnected, with the purpose of having the smallest fault current as possible. Also, the fault resistance is the same as the previous case ($R_f = 3000\Omega$).

Table 6-13. Phasors Magnitude in 100% Compensation System and High Fault Resistance

Value Source	Simulation
Compensation	100%
$3I_{0HE}$ [A]	8.5
$3I_{0SP}$ [A]	0.7
$3I_{0SA}$ [A]	11.56
I_{Coil} [A]	20.21
U_a [kV _{rms}]	20.42
U_b [kV _{rms}]	2.2
U_c [kV _{rms}]	19.85
U_0 [kV _{rms}]	10.55
I_f [A]	0.73
I_{Rp} [A]	-

Table 6-14. Phasors Angle in 100% Compensation System and High Fault Resistance

Angle Shift	Simulation
Compensation	100%
$3I_{0HE}$	-90
$3I_{0SP}$	-4.17
$3I_{0SA}$	-89.95
I_{Coil}	-90
U_a	-31.37
U_b	-163.4
U_c	34.65
U_0 REF	85.75
I_f	-163.5

The previous two tables show the results from the simulation made. It can be noticed once again that the zero sequence voltage and the zero sequence of the faulty feeder are almost in phase, giving ellipse in the next figure, and making a clear difference one more time from the healthy feeders.

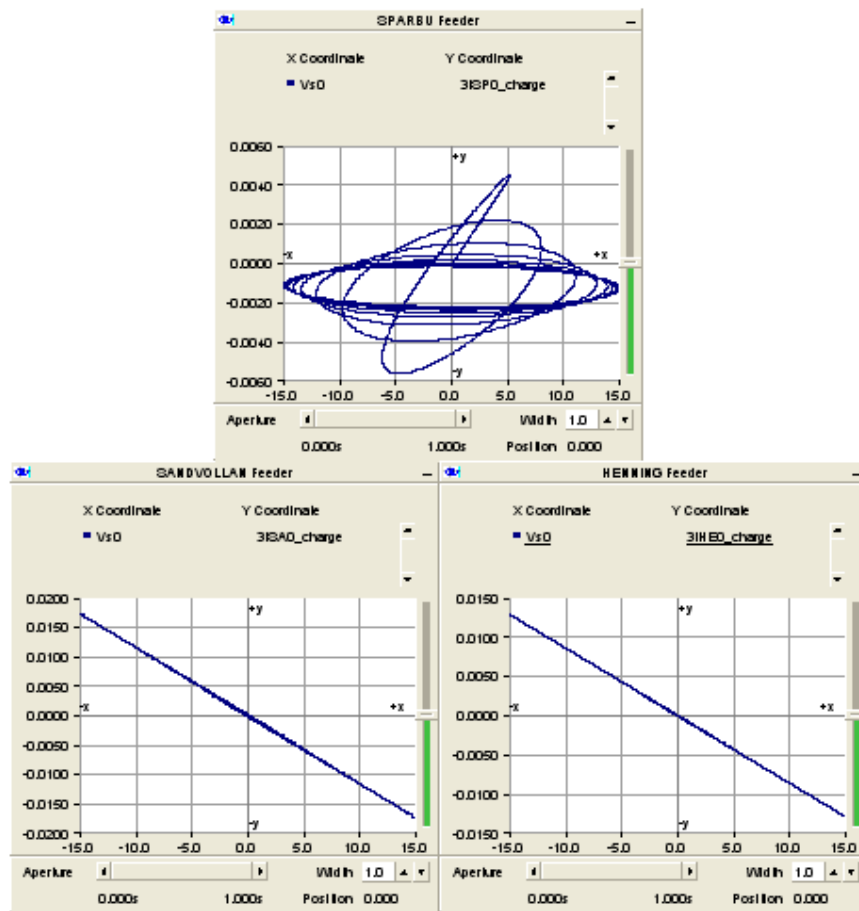


Figure 6.9. QU Diagram in 100% Compensation System and High Fault Resistance

Chapter 7

7 DISCUSSION

The principal aim of this work was the creation of a PSCAD model, pursuing a similar behavior regarding to the tested distribution network. The network, which is located near of Trondheim, was object of a field test by SINTEF and others Norwegian Companies. The report that came out from the field test served as the most important source at the moment of developing the PSCAD model. The main focus of the model was related to the magnitude, as well as the orientation of the zero sequence currents, which belongs to the feeders and the current throughout the coil. As it was told in the previous section, the capacitors were calibrated according to the mentioned zero sequence currents of the feeders in isolated condition.

At the moment of requiring a further analysis regarding the healthy feeders, it could be noticed that the angle between them and the reference (zero sequence voltage) was constant during all the cases, the reason is that the zero sequence impedance is almost entirely capacitive, coming from the ground capacitance (C_g) of the feeder. Thus, the series impedance of the overhead line could be neglected from the analysis due to the small magnitude compared with the commented ground capacitance.

It was chosen the zero sequence currents and the current throughout the coil as important parameters because of their direct relationship with the fault current, which is the subject in this work. For further explanation, the Sparbu zero sequence current involved the faulty current, and it can be appreciated due to the proximity of magnitude, as well as phase, also, the current's behavior is related to the grounding method taken in the system, all this can be notice from the previous section. Meanwhile, the little difference in the coil current between the simulations and the field test is strictly related in how it was modeled the coil, as it can be seen in the description of the substation, the coil was model ideally without any losses within, thus, a small disparity came up in the results. Nevertheless, the consistence in the results was not affected by the previous assumption.

The faulty feeder zero sequence current had a consistent behavior regarding the field whether in magnitude or angle, as it has been told in the last paragraph. In the next figure, it can be appreciated the comparison between the simulations made and the field test values of current magnitude versus all the cases previously exposed in this document.

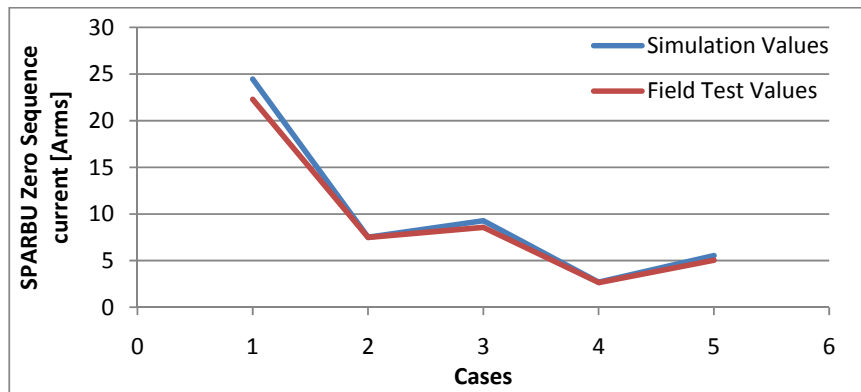


Figure 7-1. SPARBU Zero sequence current

The same action was taken regarding the current throughout the coil, which had the same pattern in the simulation as the field test values, as it can be seen as well in the next figure.

The consistence in the last two variables gives an entire validation to the proposed model for being a trustable representation of the studied real distribution network.

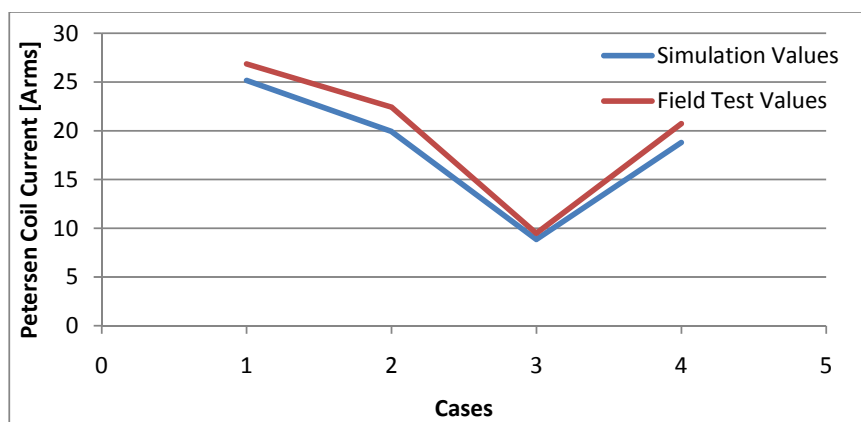


Figure 7-2. Arc Suppression Coil Current

The resonant grounding has been the focus throughout the entire document. The main advantage is the effective minimization of the fault current, this could be fully appreciated in the case of 100% compensation without parallel resistance connection exposed in the results section, and because of this, a sustained service to the customer can be given during faults. Therefore, the transient faults are automatically removed and the operation could be sustained during hours or even days, i.e. that the arcs are normally self extinguished and the fault is clear without the intervention of the fuses or switches. Nevertheless, the grounding system in treatment will give a high voltage stress, where the grounding method throughout the arc suppression Coil is implemented, and given the right circumstances like high unbalance and low damping in the system, the maximum of the resonance curve can be greater than the nominal voltage, as it can be seen from the resonance curve in the previous section, this is not the case of the studied system due to the maximum peak of the resonance curve was almost 3 kV in a 22 kV network. Moreover, a fault detection sensitivity problem is created by this grounding method, caused by the rather low fault currents, which can be confused with the unbalance in the network and the high zero sequence voltage generated. Thus, it has become a challenge for this system grounding the detection and location of faults single phase to ground faults.

In order to solve, the most important drawback of the popular resonant grounding, a location and detection method for single phase to ground faults was introduced and implemented in the PSCAD model, giving positive results after testing it throughout the simulations. The method was tested in the worst situation for detecting and locating a single phase to ground fault, when the distribution network was 100% Compensated without parallel resistance connection and the fault possessed a high resistance, then, the fault current could be detected and located, and it was given a clear difference throughout the charge - voltage diagrams, which feeder was the faulty one and which ones were healthy. Therefore, it was proved throughout real measurement and simulations the effectiveness of this new method for fault location and detection.

Chapter 8**8 CONCLUSIONS AND RECOMMENDATIONS**

The created PSCAD model can be used as an authentic representation of the distribution network tested by SINTEF and others companies in August of 2005, due to the consistency of results between the simulations and the field test.

The proposed fault detection and location method did not show any limitation regarding the studied network. Also, the gotten shapes were consistent with the diagrams gotten in the field test. It was added one special case in order to find any limitation, but it was not found any. However, any case of over compensation was not made throughout this work.

According to the problem description proposed at the beginning of the present document, the aims of this work have been fulfilled.

During the implementation of the travelling wave line model, a problem of modeling was present, because of the time step taken at that moment. The inconvenient was solved after changing the time step according to the next expression:

$$\text{time step } \Delta t = \frac{l}{c}$$

Where l represents the length of the shortest overhead line in the network and c stands for the light speed. The previous expression should be always considered, when it is desired the representation of an overhead line throughout the travelling wave model.

Throughout the QU diagram, information can be got in the case of the faulty feeder. The interval taken during the simulations for the diagrams was the entire fault time, therefore the ellipse shape, it

could not be appreciated. Thus, the time interval taken should not be bigger than three cycles in order to visualize the shape of the faulty feeder.

The Bergeron model was taken over before to the line model described in this work, and it is important to point out that the proposed detection and location method presented a limitation in the hardest case evaluated in this work, due to the not possible identification of the faulty and healthy feeders. It must be remembered that the Bergeron model works at rated frequency and it is based in the travelling wave model.

Chapter 9

9 FUTURE WORK

The presented model done in PSCAD, which was validated throughout this work, will be a valuable tool for further researches in the area of Power System, specifically, in the distribution networks. The research that could be taken place in this model could cover the following points:

- Study of distributed coil grounded neutrals.
- Over compensation studies.
- Comparison between different detection and location methods.
- Limitation studies about the proposed fault detection and location method.

10 Bibliography

- [1]. *Study of the Neutral to Ground Voltage in a Compensated Power System.* **V. Leitloff, L. Pierrat and R. Feuillet.** 2, s.l. : ETEP, 1994, Vol. 4.
- [2]. **Petersen, W.** *Neutralizing of Ground Fault Currents and Suppression of Ground Fault Arcs through the Ground Fault Reactor.* s.l. : E.T.z, 1916.
- [3]. **P. Toman, J. Orsagova and D. Topolanek.** *Location of the Earth Faults in MV Compensated Networks.* s.l. : Brno University of Technology.
- [4]. *Locating Earth Faults in Compensated Distribution Networks by means of Fault Indicators.* **E. Bjerkan, T. Venseth.** Montreal : International Conference on Power Systems Transients, 2005.
- [5]. **Feng Yan and Zengwei Guo.** *Composite Fault Location Method of Single Phase to Earth about Rural Distribution Networks.* s.l. : Noth China Electric Power University, 2009.
- [6]. *Faulty Feeder Identification Based on Charge-Voltage Relation.* **T. Heriksen, A. Petterteig.** Bergen : s.n., 2008. NORDAC.
- [7]. **Thor Henriksen and Astrid Petterteig.** *Single Phase earth fault field measurements including transients - August 2005.* Trondheim : SINTEF, 2006.
- [8]. **Petterteig, Astrid.** *Single phase earth fault field measurements including transients - presentation of additional curves.* Trondheim : SINTEF, 2006.
- [9]. **Roepfer, Richard.** *Short Circuit currents in Three Phase Networks.* s.l. : Pitman Publishing, 1972.
- [10]. **Guldbrand, Anna.** *Earth Faults in Extensive Cable Networks.* Lund : Lund University, 2009.
- [11]. *Electric Distribution Network Design.* **Lakervi E. and Holmes E.J.** 2003, IEEE Power Series 21.
- [12]. **P.M., Anderson.** *Analysis of faulted power systems.* New York : IEEE, 1995.
- [13]. **Jeff Roberts, Dr Hector J. Altuve, and Dr Daqing Hou.** *Review of Ground Fault Protection Methods for Grounded, Ungrounded, and Compensated Distribution Systems.* Washington : Schweitzer Engineering Laboratories, inc, 2001.
- [14]. **Blackburn, J. L.** *Protective Relaying: Principles and Applications.* New York : Marcel Dekker, 1998.

- [15]. *High resistance grounding*. **Bridger, B.** s.l. : IEEE Transactions on Industry Applications, 1983, Vols. IA-19.
- [16]. *Application of Resonant Grounding in Power Systems in the United States*. **Eric T. B. Gross, Edward W. Therton,** 1951.
- [17]. *Verifying Resonant Grounding in Distribution Systems*. **I. Zamora, A.J. Mazon, K.J. Sagastabeitia, O. Pico and J.R. Saenz.** 2002, IEEE Computer Applications in Power, pp. 45-50.
- [18]. *Neutral Grounding in High Voltage Transmission*. **Wilheim, R. and Walters, M.** Elsevier : s.n., 1956.
- [19]. *A new directional transient relay for high ohmic earth faults*. **G. Druml, A. Kugi and O. Seifert.** Barcelona : s.n., 2003. CIRED.
- [20]. *New adaptive algorithm for detecting low and high ohmic faults in meshed networks*. **G. Druml, W. Klein and O. Seifert.** Prague : International Conference on Electricity Distribution, 2009.
- [21]. **Ljung, L.** *System identification: theory for the user*. New Jersey : Prentice Hall PTL, 1999.
- [22]. *Control of Petersen Coils*. **G. Druml, A. Kugi and B. Parr .** Linz : s.n., 2001. International Symposium on Theoretical Electrical Engineering.
- [23]. **v4.2.1, PSCAD.** *Help Manual*. s.l. : Manitoba HVDC Research Center, 2006.
- [24]. *Reduced order transmission line models for power system analysis*. **Lefebvre, Serge.** 1999, Electrical Power and Energy Systems 21, pp. 211-223.
- [25]. **Lehtonen M. and Hakola T.** *Neutral earthing and power system protection - Earthing solutions and protective relaying in Medium Voltage Distribution Networks*. Vaasa : ABB Transmit Oy, 1996.
- [26]. *Planleggingsbok for Krafnett, Bind III*. Trondheim : SINTEF, 2003.
- [27]. **Henriksen, Thor.** *Faulty Feeder Identification based on Charge Voltage Relation*. Trondheim : SINTEF, 2008.

APPENDIX A

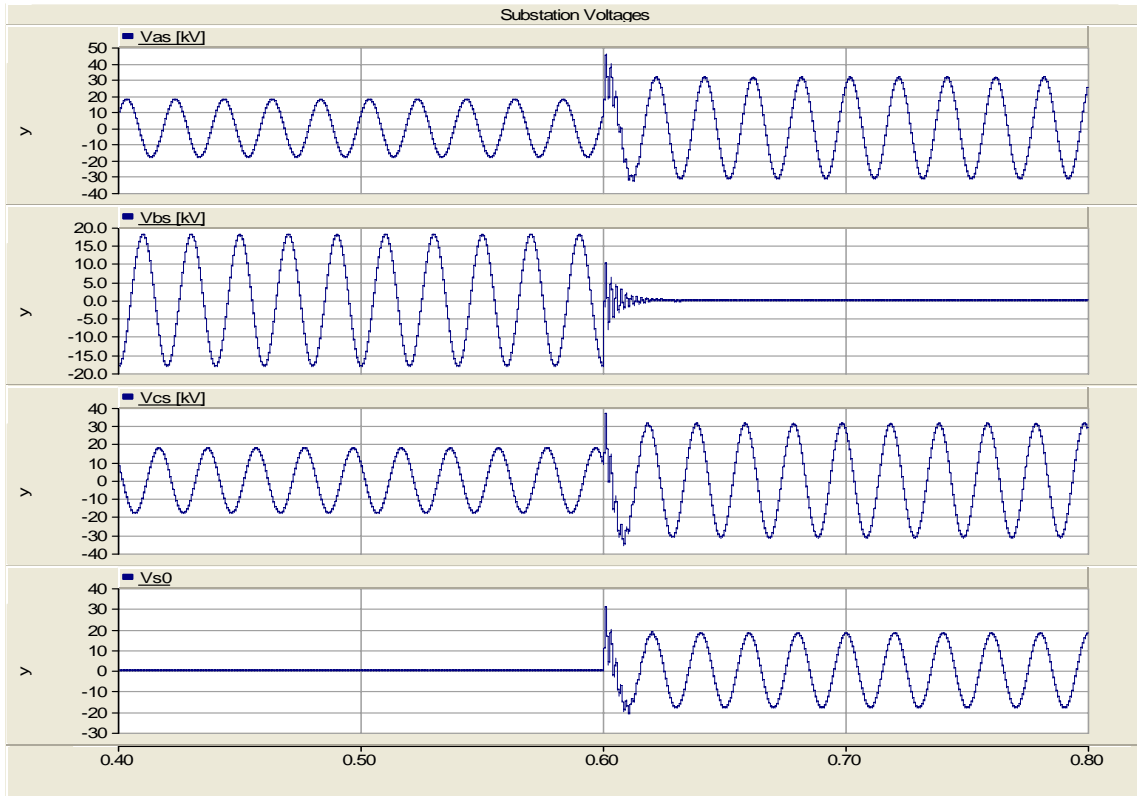


Figure A-1. Substation Voltages in Isolated Condition

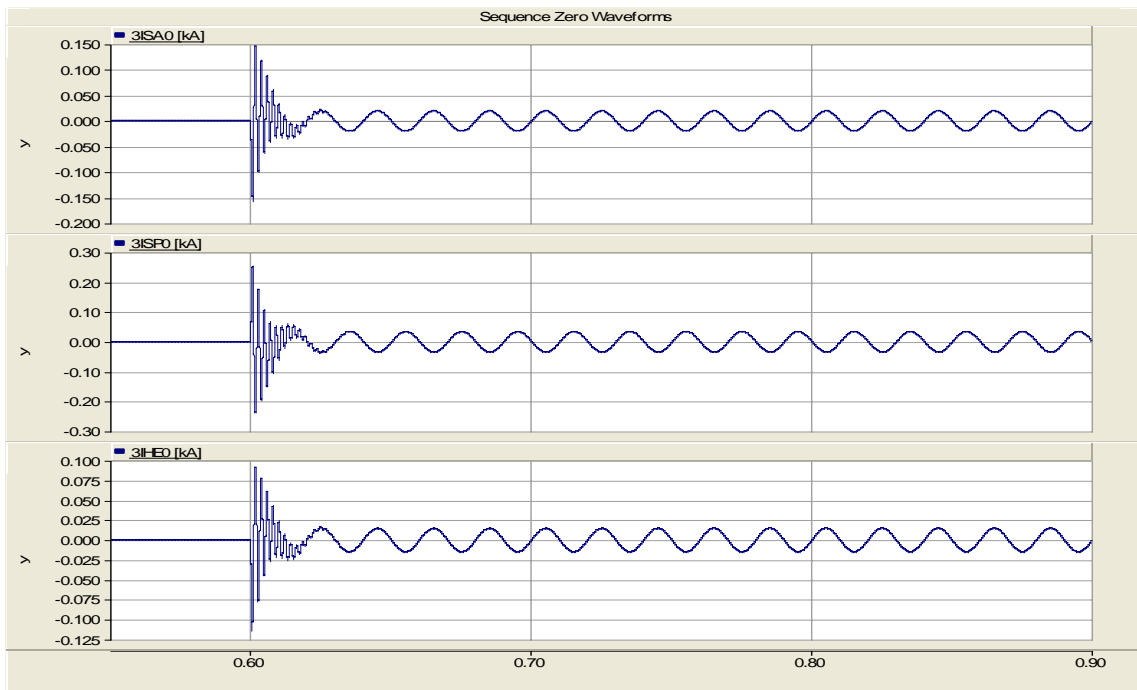


Figure A-2. Zero sequence currents in Isolated Condition

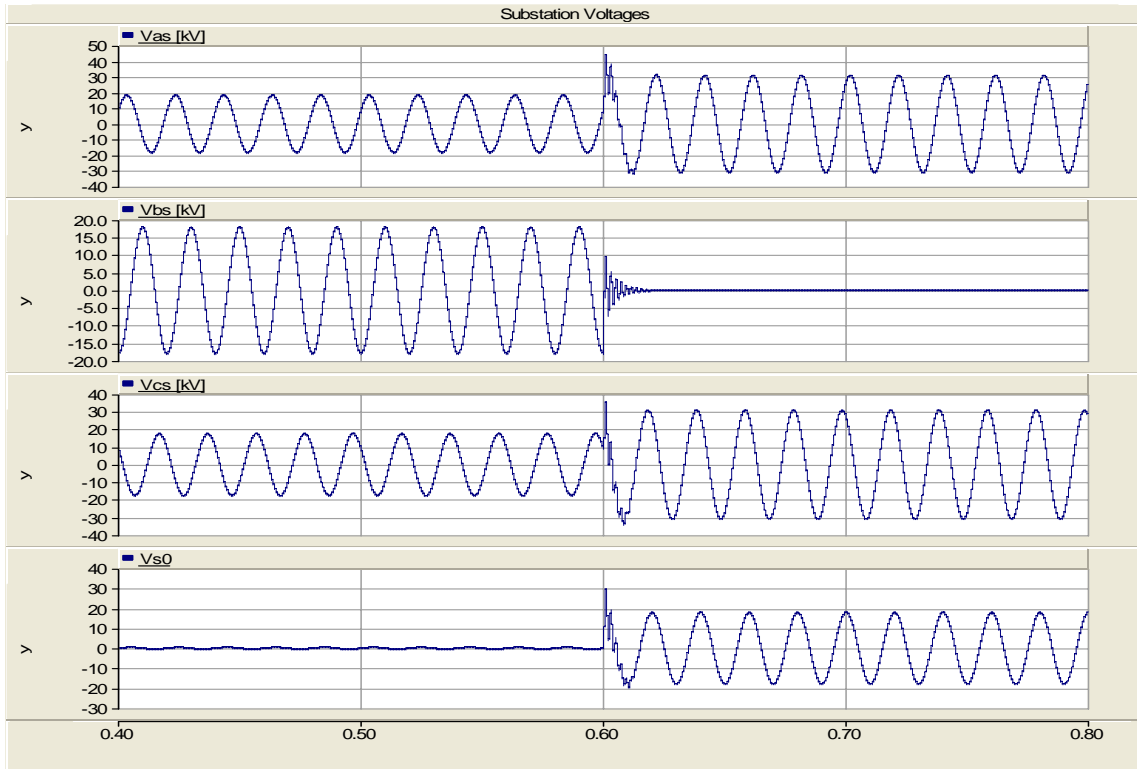


Figure A-3. Substation Voltages in 100% Compensation with Parallel Resistance Connection

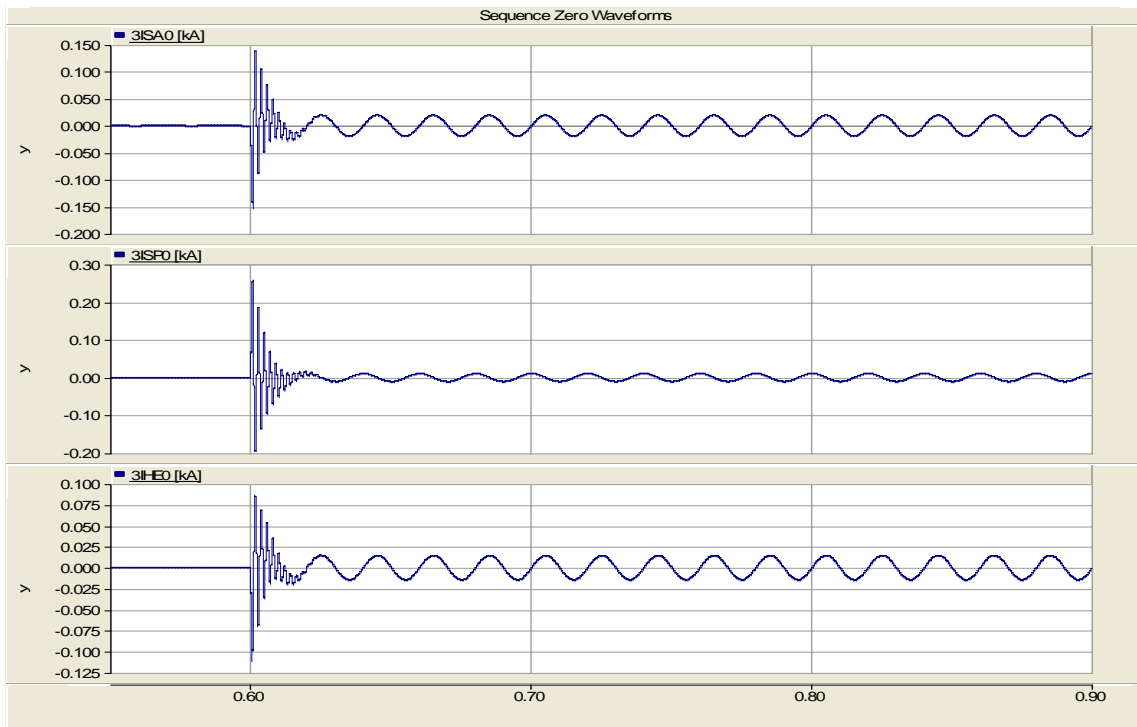


Figure A-4. Zero sequence currents in 100% Compensation with Parallel Resistance Connection

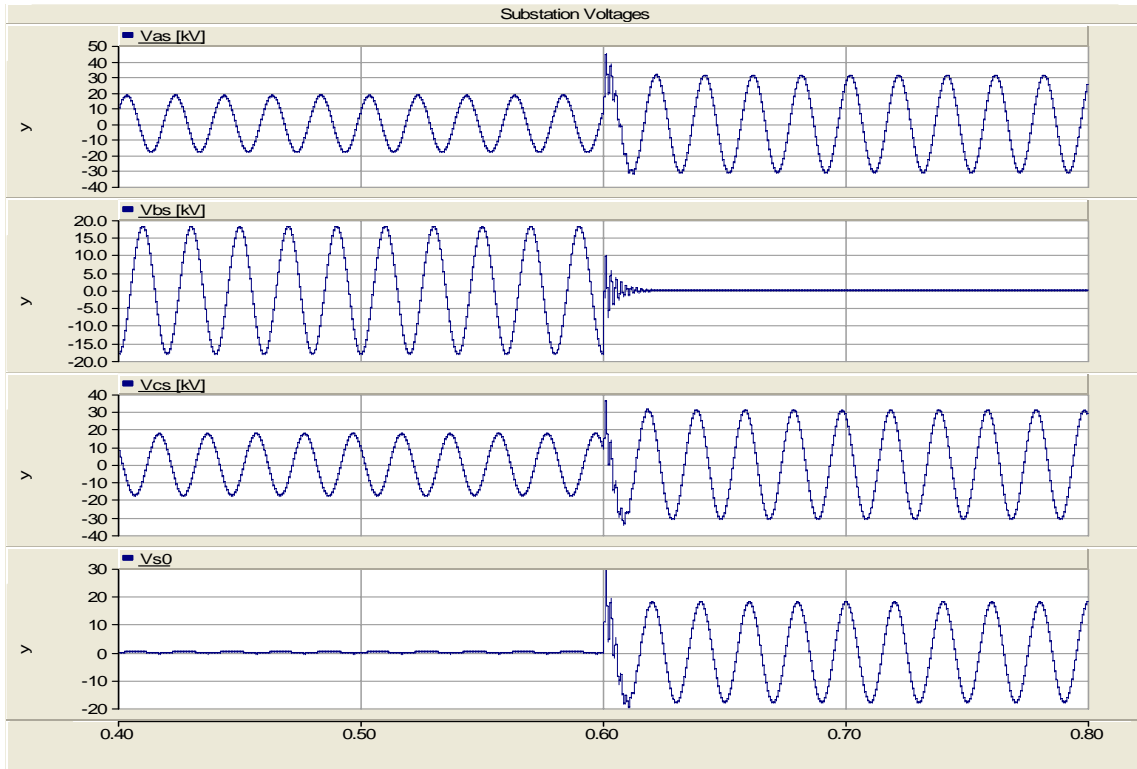


Figure A-5. Substation Voltages in 80% Compensation with Parallel Resistance Connection

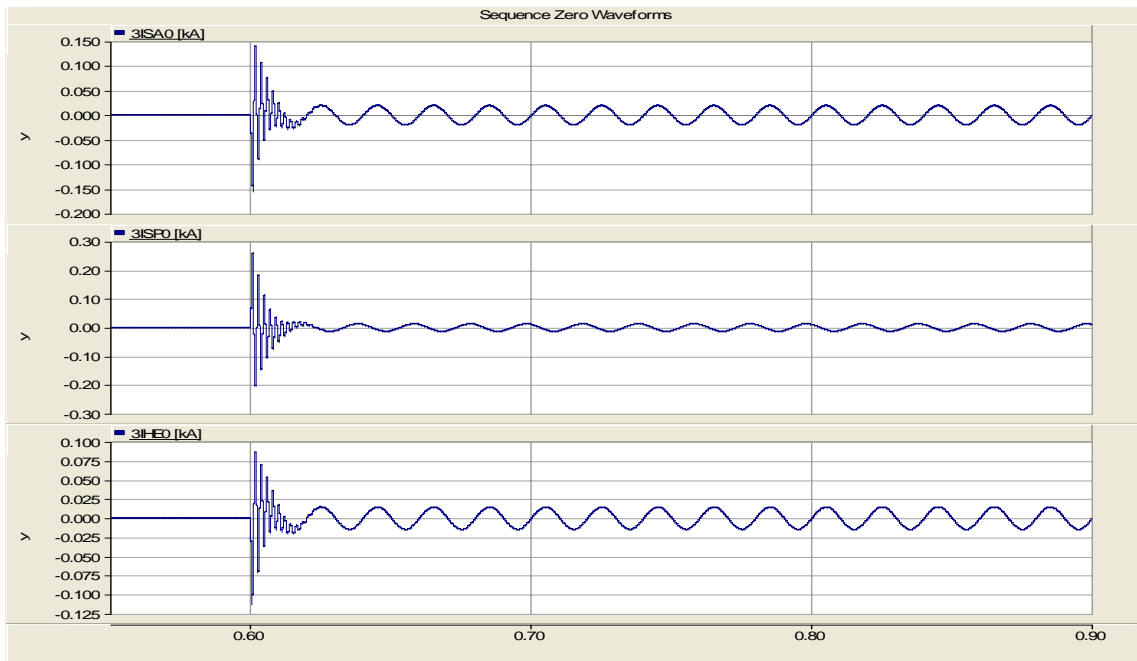


Figure A-6. Substation Voltages in 80% Compensation with Parallel Resistance Connection

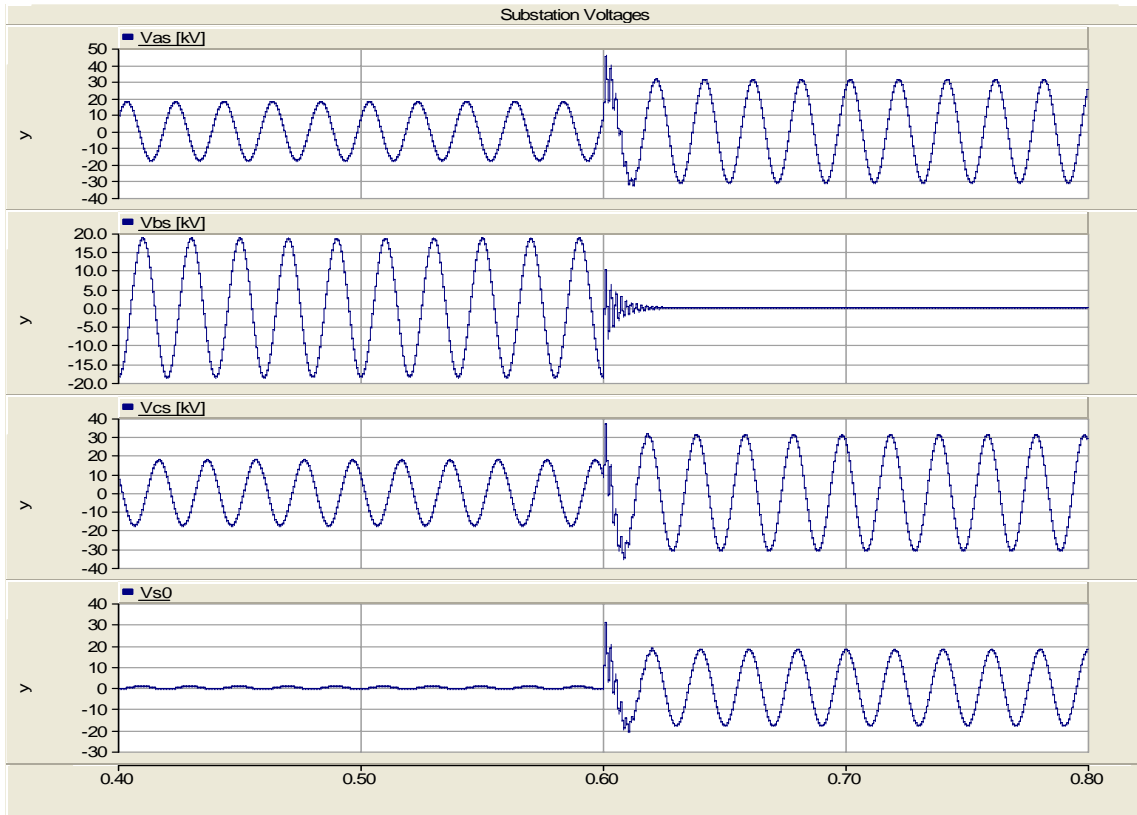


Figure A-7. Substation Voltages in 80% Compensation System

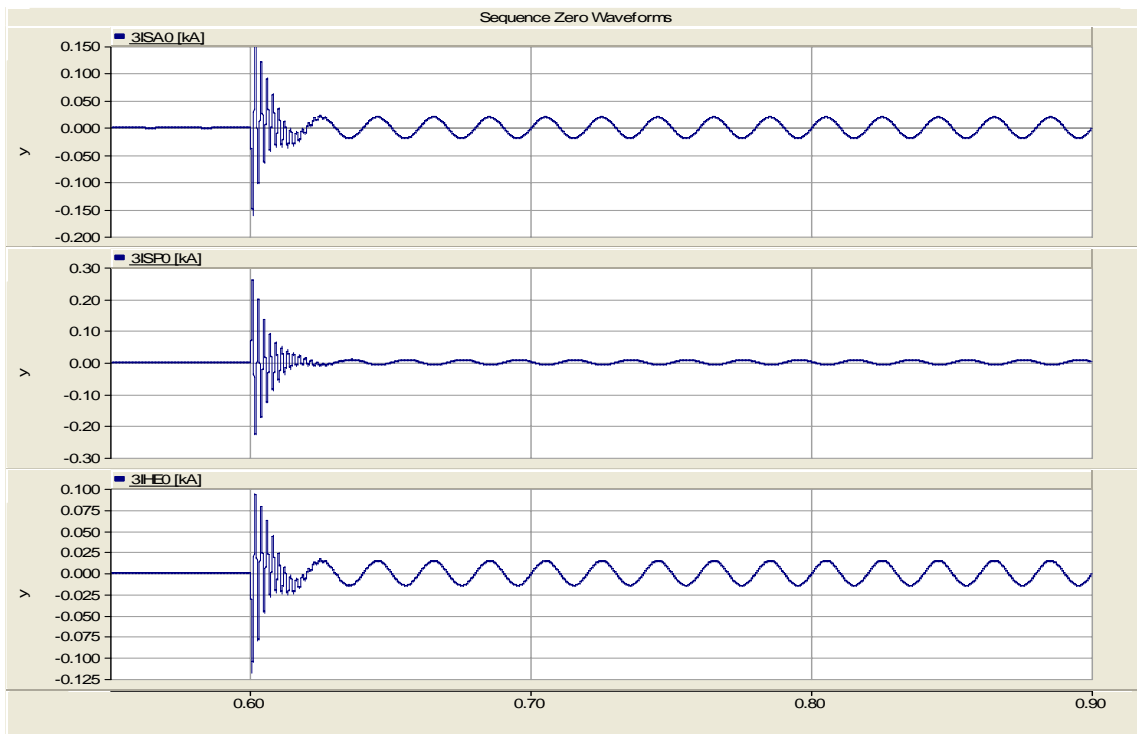


Figure A-8. Zero sequence currents in 80% Compensation System

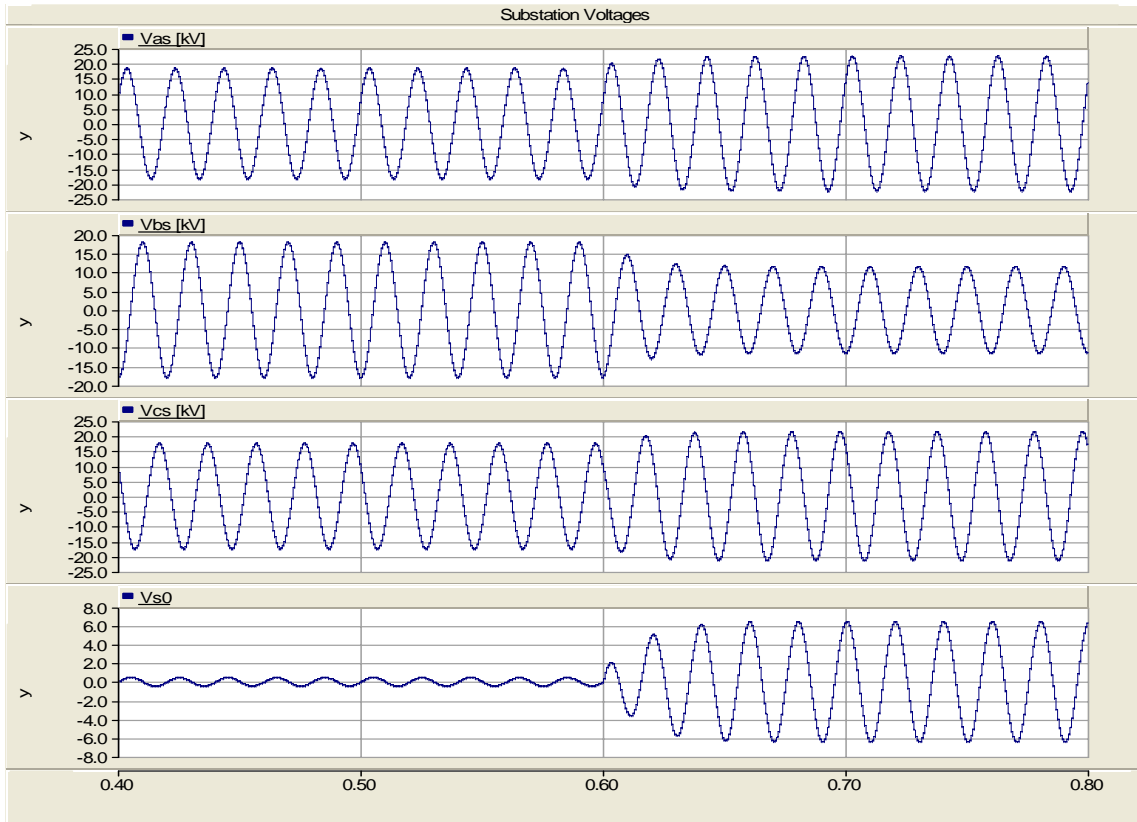


Figure A-9. Substation Voltages in 80% Compensation with Parallel Resistance Connection and High Fault Resistance

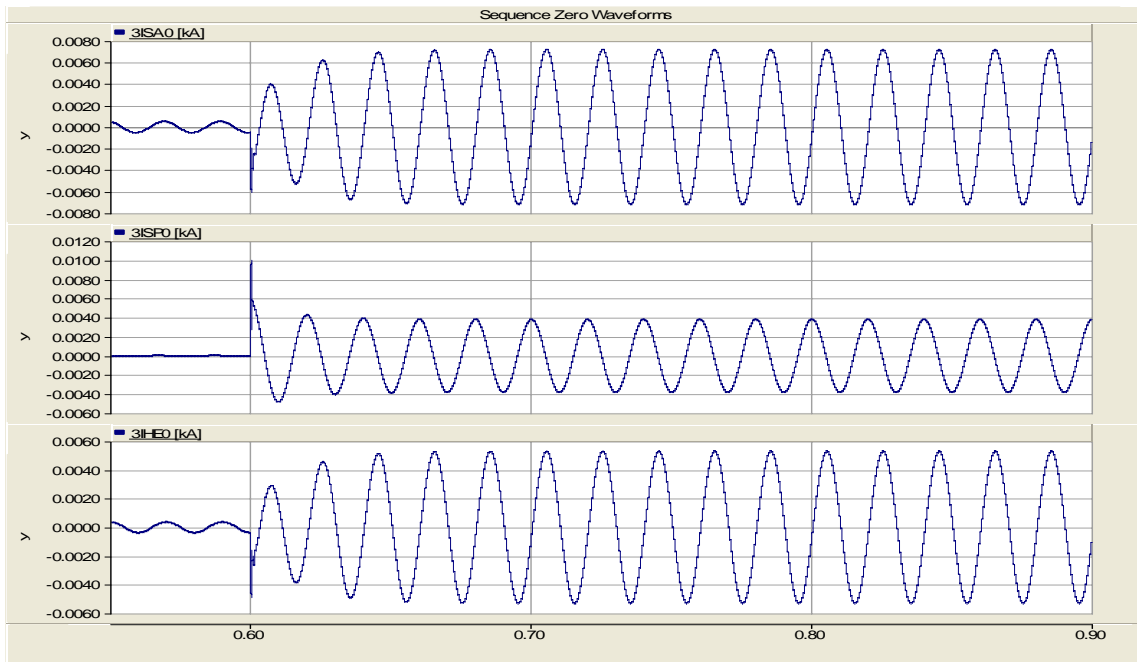


Figure A-10. Zero sequence currents in 80% Compensation with Parallel Resistance Connection and High Fault Resistance

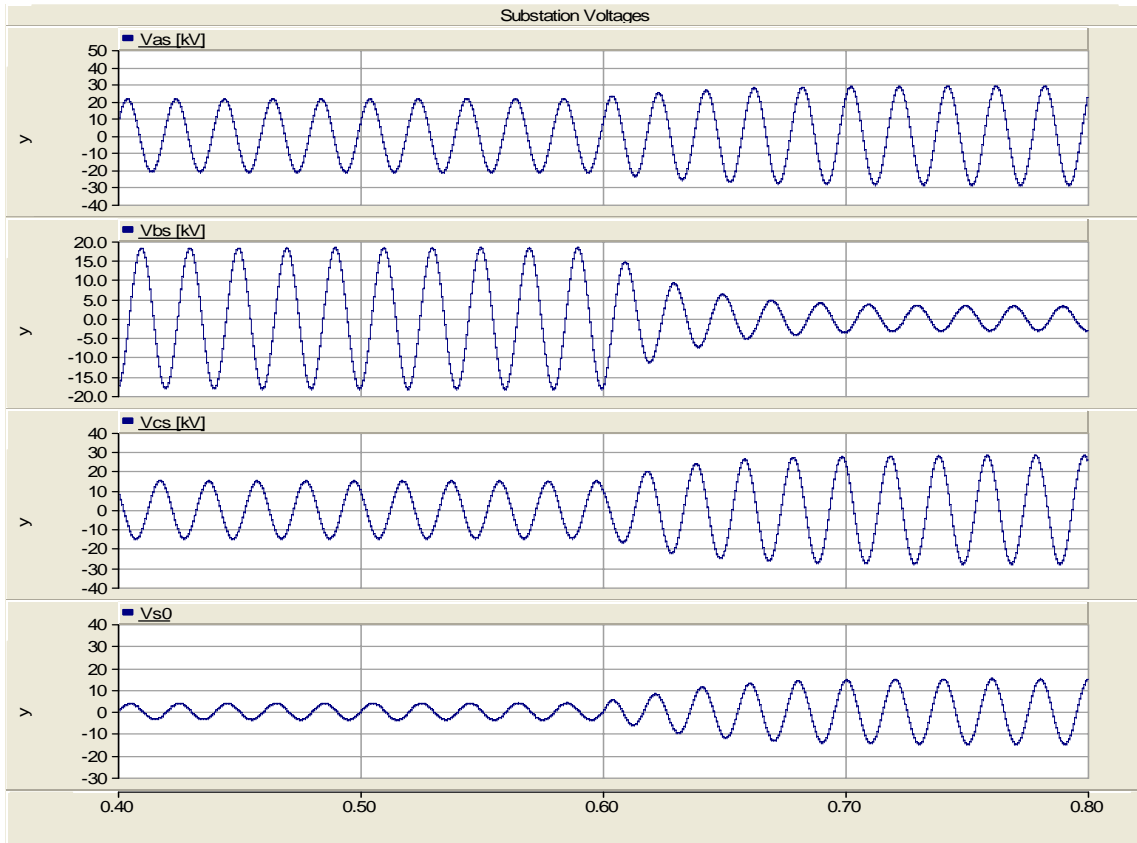


Figure A-11. Substation Voltages in 100% Compensation System and High Fault Resistance

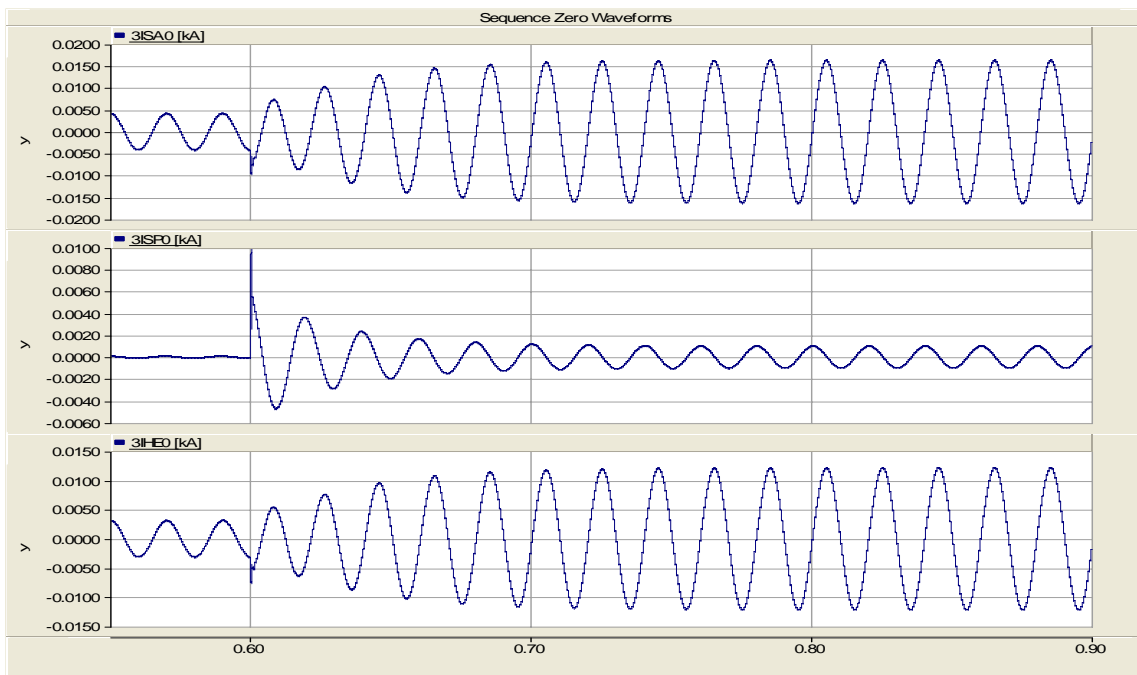


Figure A-12. Zero sequence currents in 100% Compensation System and High Fault Resistance